

ABSTRACT

Title of Document: THE CORE OF EUKARYOTIC RIBOSOMAL
PROTEIN US19 FUNCTIONS AS A PIVOT
POINT ENHANCING RIBOSOME
FLEXIBILITY

Alicia Marie Bowen, Doctor of Philosophy, 2015

Directed By: Professor Jonathan D. Dinman, Department of
Cell Biology and Molecular Genetics

While most ribosomal elements are highly conserved in the three domains of life, over the course of evolution, significant differences have emerged as ribosomes have been subjected to different types of selective pressure. In prokaryotes and archaea, a single small subunit protein, uS13, partners with H38 (the A-site finger) and uL5 to form the B1a and B1b/c bridges, respectively. In eukaryotes, it appears that the small subunit component was split into two separate proteins during the course of evolution. One of these, also known as uS13 (previously known as S18), only participates in bridge B1b/c with uL5 in eukaryotes (previously known as L11). The other, called uS19 (previously known as S15) is the small subunit partner in the B1a bridge with H38. Here, poly-alanine mutants of the uS19/Us13 interface of uS19 were used to elucidate the evolutionary advantage of this split. A previously described chemical protection profile of the B7a bridge was utilized in order to determine the ribosomal rotational status of the selected mutants. rRNA structure probing analyses reveal that uS19/uS13 interface mutations shift the ribosomal rotational equilibrium toward the unrotated state. This

perturbation of ribosomal rotational equilibrium also affected the ribosomes affinity for two intrinsic ligands: unrotated ribosomes exhibit increased affinity for ternary complex and disfavor binding of the translocase, eEF2. We posit that this mutation causes the normally flexible head region of the small subunit to “stiffen”, thereby decreasing the ribosomes range of motion. A model is presented in which residues L₁₁₂GH₁₁₄ at the uS19/uS13 interface act as the ball in a “ball-and-socket joint”, providing the increased flexibility required in the head region of the eukaryotic SSU as a consequence of the evolutionary process.

THE CORE OF EUKARYOTIC RIBOSOMAL PROTEIN US19 FUNCTIONS AS
A PIVOT POINT ENHANCING EUKARYOTIC RIBOSOME FLEXIBILITY

By

Alicia Marie Bowen

Dissertation submitted to the Faculty of the Graduate School of the
University of Maryland, College Park, in partial fulfillment
of the requirements for the degree of
Doctor of Philosophy
2015

Advisory Committee:
Professor Jonathan D. Dinman, Chair
Associate Professor Kwaku Dayie
Associate Professor Douglas Julin
Associate Professor Nicole LaRonde-LeBlanc
Professor Leslie Pick

Dedication

First of all, I dedicate this to my late grandfather, Dee Benjamin Waller, my first teacher. You took notice when, at 4 years old, I was already reading newspapers and chapter books. You bought me that little yellow table, workbooks, and a composition notebook and gave me my first glimpse into formal education. You were “Mr. Dee” during school time and “Grandpa” the rest of the time, and my older cousins still tease me for refusing to acknowledge that you two were one and the same. You supplied us with our first computer and printer and taught us everything we needed to know about them. And even since your passing, you have continued to be my motivation to learn as much as possible. I miss you and I hope you know that all of this has been for you.

Finally, I dedicate this to anyone who knows how it feels to have nothing to eat, and nowhere to live. I dedicate this to anyone who has ever been not just a witness of eviction, but a victim. I dedicate this to you if high school counselors suggested that you were better off not going to college ...if I did it, so can you.

Acknowledgements

First and foremost, I acknowledge that I do not have the strength or discipline to have made it this far alone. All glory and honor belongs to God.

Thank you Dr. Dinman for EVERYTHING. We joke that you are like a therapist, but the truth is that you're better than a therapist because you don't charge for your services. Thank you for never giving up on me, for all of the jokes, for understanding me [at times, better than I understood myself], and for encouraging me along the way.

Thank you to my committee members for your support through the years. I truly appreciate your guidance.

Thank you to my mentors: Dr. Duncan Quarless, Dr. Robert Hoyte, and Mrs. Kia Davis. I wouldn't have made it to college or applied to graduate school without your positive influence.

Thanks to my parents, Sandra and Linden Munroe. Mom: We've had our struggles through the years, but we made it through as a unit. Thank you for every encouraging word, for being my cheerleader, for letting me cry to you on the phone when things got rough, and for celebrating every victorious moment with me as if it were your own.

I would like to thank my siblings: Ashley, Edwin, Andrew, Avery, and Asia (and Trina). I don't want to go through life without any of you. Thank you for every laugh, every smile, every dance, every inside joke, every hug, every phone call, every text... I couldn't have made it this far without my big, supportive family.

Thank you to my extended family and in-laws. There are too many to name, of course, but please know that each of your names is written on my heart and I thank you for always encouraging me, checking up on me, providing for me, and loving me.

I could not have made it through graduate school without my friends who are a second family. My NOBCChE family: Dr. Domonique Downing, Dr. Rennisha Wickham, and Dr. Chris Sims. I appreciate our unique bond and all of the positive reinforcement. Thank you to my graduate school best friend, Colef Talbert. My childhood best friends: Jessie Brewer, Brandon Carroll, Portia Silvera, and Amelia Stevenson. Thank you all for your friendships and for all of the laughs (and for letting me write my thesis in your respective homes)!

I would like to thank all past & present members of the Dinman lab. Specifically, thank you Dr. Sharmishtha Musalgaonkar, Dr. Suna Gülay, Cassie Moomau, and Carol Vieira for the rich friendship that has extended far beyond the walls of the lab.

Finally, I would like to thank my husband, Antoine Cheek. Thank you for all of the love and encouragement and for remaining sweet and loving during the times when graduate school drove me crazy.

Table of Contents

Dedication	ii
Acknowledgements	iii
Table of Contents	v
List of Figures	vii
List of Abbreviations	ix
Chapter 1: Introduction	1
Ribosome Structure	1
The LSU	3
The SSU	4
Ribosomal RNA Interactions	5
Ribosome Biogenesis	7
Eukaryotic Translation	12
Initiation	12
Elongation	15
Termination and Recycling	19
Translational Recoding	22
Programmed -1 Frameshifting	22
Programmed +1 Frameshifting	25
Missense and Nonsense Codon Suppression	27
Small Molecule Translation Inhibitors	28
Ribosomal Proteins uS19 and uS13	29
Research Overview	33
Chapter 2: Ribosomal Protein uS19 (S15)	34
Introduction	34
Results	37
Mutant viability screen reveals inviable uS19-uS13 interface mutants	37
LGH112-114 mutant exhibits pronounced temperature and drug sensitivity	39
uS19-uS13 interface mutations alter translational fidelity	41
uS19-uS13 interface mutants exhibit a ligand binding profile indicative of unrotated ribosomes	45
uS19/uS13 dimer interface mutants perturb the rotational equilibrium of ribosomes	47
Discussion	48
Chapter 3: Materials and Methods	54
Strains, plasmids, and media	54
Genetic Assays	54
Quantitative Translational Fidelity Assays	55
Ribosome Purification	56
Ligand Binding Assays	57

Ribosomal RNA Chemical Modification and Analysis.....	59
Molecular RNA (mRNA) Abundance Assay.....	60
Chapter 4: Conclusions and Future Directions	61
Medical Impact:.....	62
Future Directions:.....	63
Appendix 1: List of Synthetic Oligonucleotide Primers.....	64
Appendix 2: Yeast Strain List.....	66
Appendix 3: Genetic and Functional Analyses of B1a Bridge Mutants in uS19	68
Bibliography.....	71

List of Figures

Figure 1: Eukaryotic Ribosome Structural Elements.....	2
Figure 2: Locations of Intersubunit Bridges.....	2
Figure 3: 60S Subunit (LSU).....	4
Figure 4: 40S Subunit (SSU).....	5
Figure 5: 80S Ribosome.....	7
Figure 6: Pre-rRNA Processing During Ribosome Biogenesis.....	9
Figure 7: Model of Ribosomal Subunit Assembly.....	11
Figure 8: Overall Process of Canonical Eukaryotic Translation Initiation.....	14
Figure 9: Model of Eukaryotic Translation Elongation Cycle.....	19
Figure 10: Eukaryotic Translation Termination and Recycling Overview.....	22
Figure 11: Programmed ribosomal frameshifting in viruses.....	24
Figure 12: General Mechanism for -1 PRF.....	25
Figure 13: Example of a +1 PRF Mechanism.....	27
Figure 14: Structures of Anisomycin & Paromomycin.....	29
Figure 15: Location of uS13 and uS19 in the 80S Ribosome & 40S Subunit.....	31
Figure 16: Locations of uS19-uS13 Interface Mutants.....	38
Figure 17: Genetic Analyses.....	40
Figure 18: Frameshifting Assay Design.....	42
Figure 19: Results from Bicistronic Reporter Assays for -1 and +1 Programmed Ribosomal Frameshifting.....	43
Figure 20: Results from Dual Luciferase Assays for Missense and Nonsense Codon Suppression.....	44

Figure 21: uS19/uS13 dimer interface mutants promote increased TC binding and decreased translocase binding	46
Figure 22: Results from hSHAPE structure probing of the B7a bridge	48
Figure 23: Residues L ₁₁₂ GH ₁₁₄ act as the “ball” in a “ball-and-socket joint” providing added flexibility to the head region of the SSU	51

List of Abbreviations

1M7	1-methyl-7-isatoic anhydride
aatRNA	Aminoacyl transfer RNA
ac-aatRNA	Acetylated aminoacyl transfer RNA
ASF	A-site finger
A-site	Aminoacyl site
ASL	Anticodon stem loop
ATP	Adenosine triphosphate
cDNA	Complementary deoxyribonucleic acid
CFU	Colony forming unit
DBA	Diamond Blackfan Anemia
eEF	Eukaryotic elongation factor
eIF	Eukaryotic initiation factor
eRF	Eukaryotic release factor
E-site	Exit site
FRET	Förster Resonance Energy Transfer
GTP	Guanosine triphosphate
hSHAPE	High-throughput 2'-hydroxyl acylation analyzed by primer extension
LSU	Large subunit
mRNA	Messenger ribonucleic acid
ORF	Open reading frame

PABP	Poly-adenosine Binding Protein
PIC	Pre-initiation complex
Pol	Polymerase
PRF	Programmed ribosomal frameshifting
P-site	Peptidyl site
PTC	Peptidyltransferase center
qRT-PCR	Quantitative Real-Time Polymerase Chain Reaction
RF	Release factor
RP	Ribosomal protein
rRNA	Ribosomal ribonucleic acid
SRL	Sarcin ricin loop
SSU	Small Subunit
tRNA	Transfer ribonucleic acid

Chapter 1: Introduction

The ribosome is a large ribonucleoprotein particle responsible for the synthesis of proteins from genetic material encoded in messenger ribonucleic acids (mRNAs). This process, termed “translation”, is an essential process for all living organisms. In recent years, several research groups have uncovered critical information about ribosome structure. In 2009, the Nobel Prize was awarded to three x-ray crystallographers responsible for solving ribosome structures.¹⁻³ This pivotal research in the translational control field provided high-resolution structural context to ribosomal processes. With the introduction of atomic-resolution structures, the focus has shifted to determining how small-scale structural components and conformational changes play into the overall complex structure and dynamics of the ribosome.

Ribosome Structure

Eukaryotic ribosomes are composed of two subunits which consist of four ribosomal RNA (rRNA) molecules and 79 ribosomal proteins (Figure 1). The rRNA molecules (5S, 5.8S, 18S, and 25S) and ribosomal subunits (40S and 60S) are named for their sedimentation coefficients. The large subunit or LSU (50S in prokaryotes; 60S in eukaryotes) consists of 47 ribosomal proteins and three rRNA molecules. The small subunit or SSU (30S in prokaryotes; 40S in eukaryotes) contains 32 ribosomal proteins and an 18S rRNA molecule. During the process of protein synthesis, the large and small ribosomal subunits are held together by interacting regions known as intersubunit bridges. (Figure 2) Roles of these bridges range from aiding subunit association to transmitting signals between functional centers of the ribosome.⁴ Of the 17 intersubunit

bridges in eukaryotic ribosomes, 8 involve protein-rRNA interactions and only 2 involve protein-protein interactions.⁵

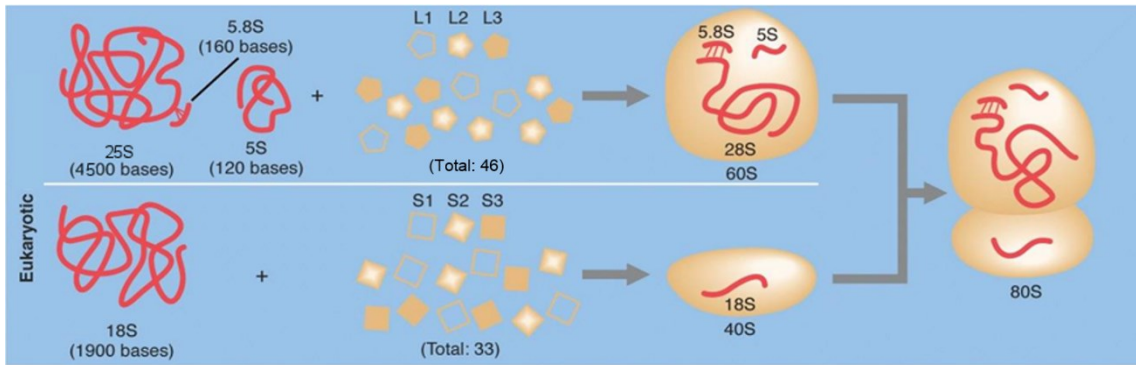


Figure 1: Eukaryotic Ribosome Structural Elements.

Ribosomal RNA, proteins, and subunits represented. Image from Molecular Cell Biology (Lodish)⁶

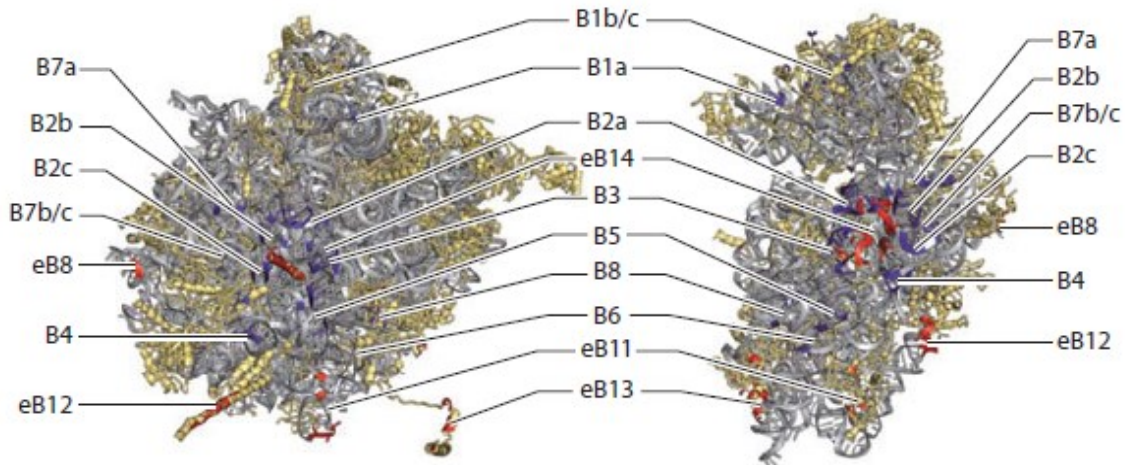


Figure 2: Locations of Intersubunit Bridges

View from the intersubunit face of the large (left) and small (subunits) with all bridges labeled. Image from Yusupov et al (2012)⁷

The LSU. The LSU contains the peptidyltransferase center (PTC), the site of peptide bond formation (Figure 3). While both subunits harbor three tRNA binding sites called A- P- and E-sites, the bulk of the tRNAs interact with the LSU. The aminoacyl (A) site is the location where all tRNAs sample the incoming codon. Directly 5' to the A-site is the peptidyl (P) site. This is the tRNA binding pocket that harbors aminoacylated tRNA. The exit (E) site is the final stop for tRNAs before they depart the ribosome in their newly deacylated state. Also present on the LSU are the sarcin-ricin loop (SRL), GTPase associated center, and central protuberance. The SRL is an rRNA loop on Helix 95. As part of the GTPase associated center (the P stalk is also part of this functional center), the SRL interacts with trans-acting factors (GTPases specifically) during each stage of translation. The top of domains I and II of the 5S rRNA, L5, and L11 form the central protuberance. This center serves as a contact point between the large and small subunits through intersubunit bridges B1a and B1b/c and undergoes large scale structural rearrangements during translation.

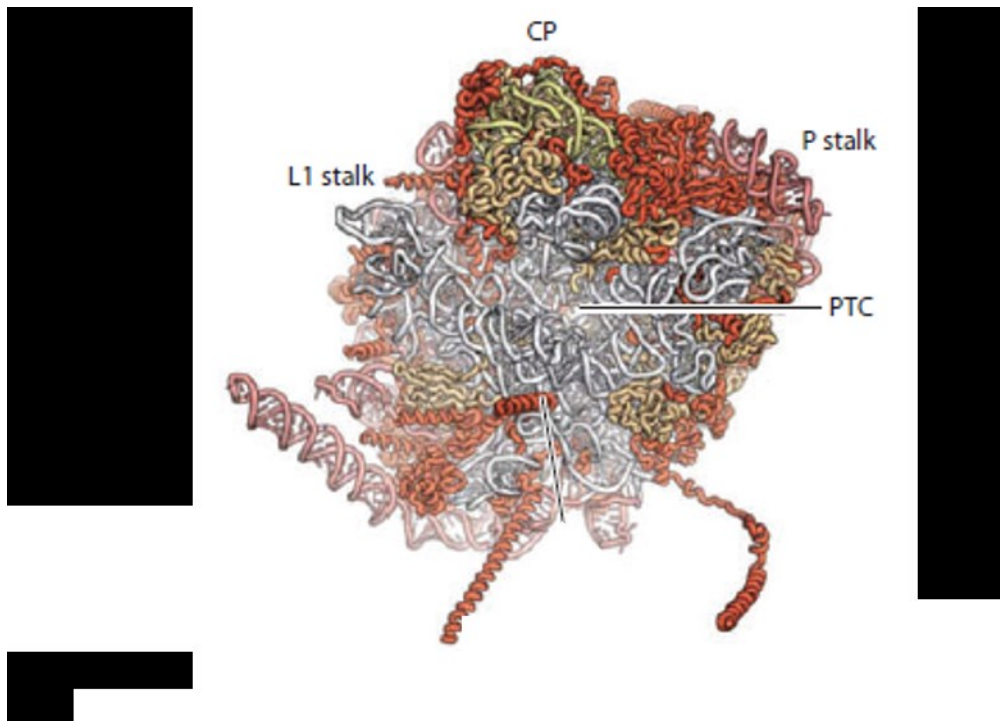


Figure 3: 60S Subunit (LSU).

Crown view of the LSU. Central protuberance (CP), P Stalk, L1 Stalk, and peptidyl transferase center (PTC) are labeled. Image modified from Yusupov, et al (2012)⁷

The SSU. Perhaps the most important structural feature of the SSU (Figure 4) is the platform. This is the stage for messenger RNA (mRNA) transcripts and also the location of the A, P, and E sites of the SSU. Base pairing between the incoming tRNA and the mRNA occurs in the decoding center. This base pairing induces the formation of a mini-helical structure between the anticodon stem loop (ASL) of the tRNA and the A-site codon of the mRNA. Upon formation of this minihelix, 18S rRNA bases A1755, A1756, and G577 (*E. Coli* A1492, A1493, and G530) swing into an open conformation, hydrogen bonding with and stabilizing the minihelix.⁸ The SSU undergoes additional conformational changes throughout translation. The head region (labeled H in Figure 4)

which contains the B1a and B1b/c bridges, rotates at the neck domain by 14° with respect to the rest of the small subunit during subunit rotation.^{9,10} Recently, a eukaryote-specific motion was identified wherein the small subunit “rolls” orthogonal to the intersubunit rotation plane, between the pre- and post-translocational states of translation.¹¹

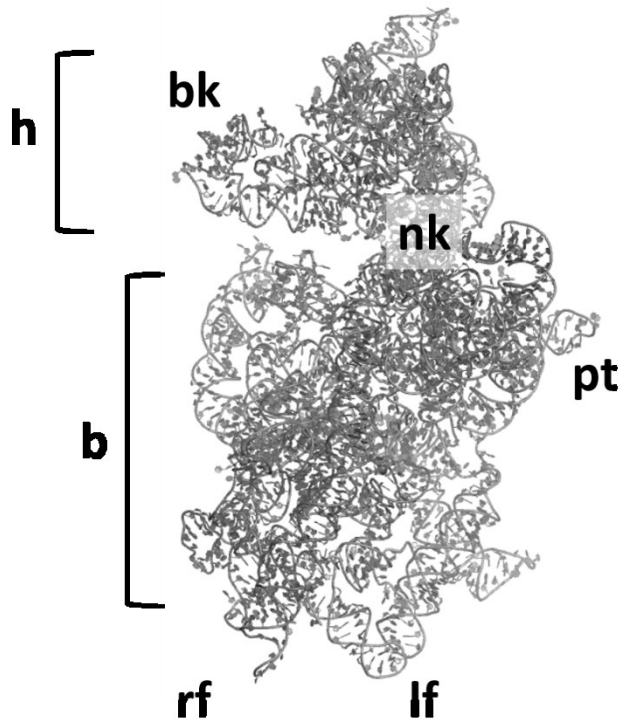


Figure 4: 40S Subunit (SSU).

40S viewed from the subunit interface. Body parts labeled: beak (bk), head (h), body (b), neck (nk), platform (pt), right foot (rf), and left foot (lf). Image created in PyMol from Yusupov, et al (2011)¹²

Ribosomal RNA Interactions. High resolution structures have highlighted the complex architecture of ribosomes and helped us to understand how so many proteins and rRNA molecules are able to come together to form very consistent shapes and

interactions between elements. Prior to solving these structures, it was unclear whether the rRNA served only as a structural scaffold or if it participated in the catalytic activity of the ribosome. With the structures, we now know that the rRNA both supports the structure of the ribosome and is directly involved in ribosome function. The rRNA is the primary component of the functional centers of the ribosome while the proteins are largely localized to the periphery (Figure 5).¹² As far as structure is concerned, the rRNA molecules participate in a vast number of non-canonical base pairing interactions in order to hold the large structure together. One example is known as the A-minor motif. A-minor interactions are precise minor groove lock-and-key interactions between an adenosine and a Watson-Crick base pair. These interactions are some of the most abundant long-range interactions found in rRNA.¹³ Helix-helix interactions are also formed by “ribose zippers” involving hydrogen bonding between the 2'-OH of a ribose in one helix and the 2'-OH and 2-oxygen of a pyrimidine (or 3-nitrogen of a purine) in another helix. These and other RNA-RNA interactions stabilize the packing of the rRNA helices into large, globular structures. Taken together, these structural elements allow the ribosome to participate in translation in a very complex yet precise and orderly manner.

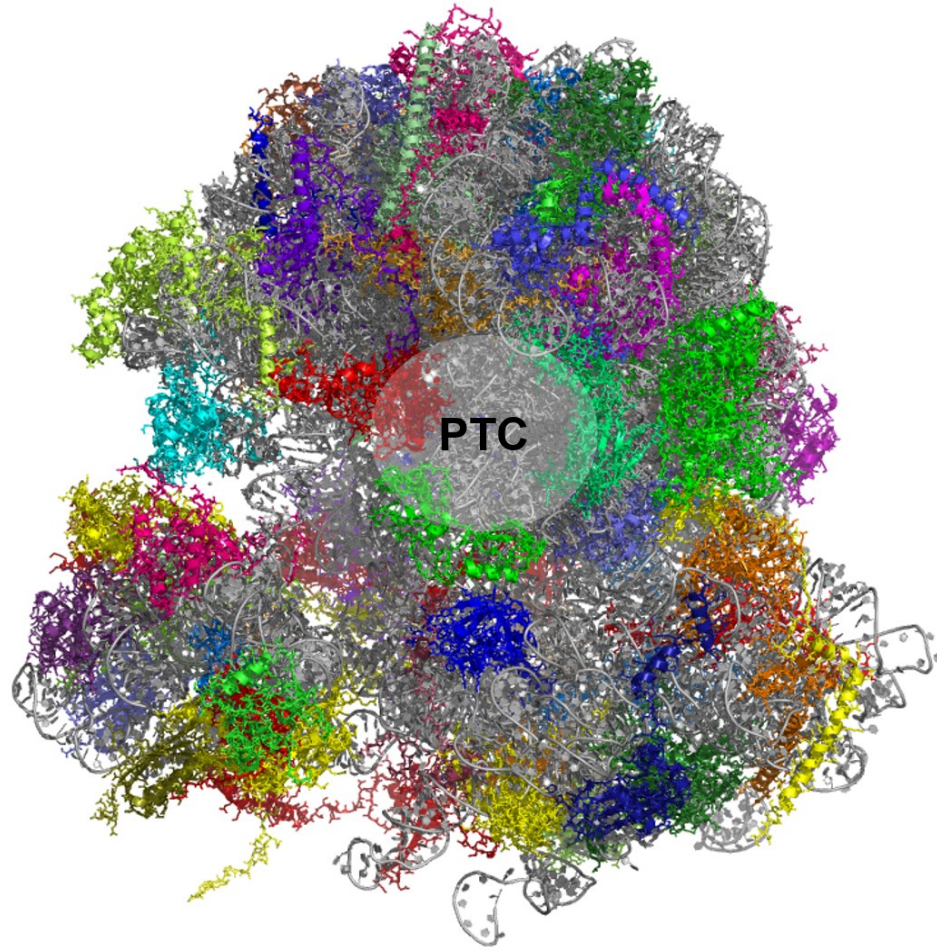


Figure 5: 80S Ribosome.

Ribosomal RNA is shown in gray and ribosomal proteins are colored. Peptidyl transferase center (PTC) is labeled. Image created in PyMol from Yusupov, et al (2011)¹²

Ribosome Biogenesis

How ribosomes are formed from the convergence of rRNA and ribosomal proteins is a complex and regulated process. The most commonly utilized model eukaryotic organism to understand this is the budding yeast *Saccharomyces cerevisiae*. Figures 6 and 7 outline the highly ordered process of ribosome biogenesis in yeast. The first steps of rRNA processing occur in the nucleolus. RNA Pol I transcribes the 35S pre-

rRNA which contains the sequences for 25S, 5.8S, and 18S rRNAs; two external transcribed spacers (ETS); and two internal transcribed spacers (ITS). A variety of chemical modifications are performed on the pre-rRNA guided by small nucleolar RNAs (snoRNAs) which base pair with the target sites to correctly position modification enzymes on the transcript. The most prevalent rRNA chemical modifications are 2'-O-ribose methylations and pseudouridylation of uridine residues. The 35S pre-rRNA also undergoes a series of cleavages (Figure 6): in the 5' ETS, the rRNA is cleaved at the A₀ and A₁ sites, and in ITS1, the rRNA is cleaved at the A₂ site. These cleavages effectively remove the 5' ETS and form the 20S and 27S precursor rRNAs. The 20S pre-rRNA is transferred to the cytoplasm where it is cleaved at site D to form the mature 18S rRNA. In parallel, the 27S pre-rRNA is cleaved in a multi-step process, to yield mature 5.8S and 25S rRNA molecules. The 5S rRNA is transcribed, independently, by RNA Pol III.

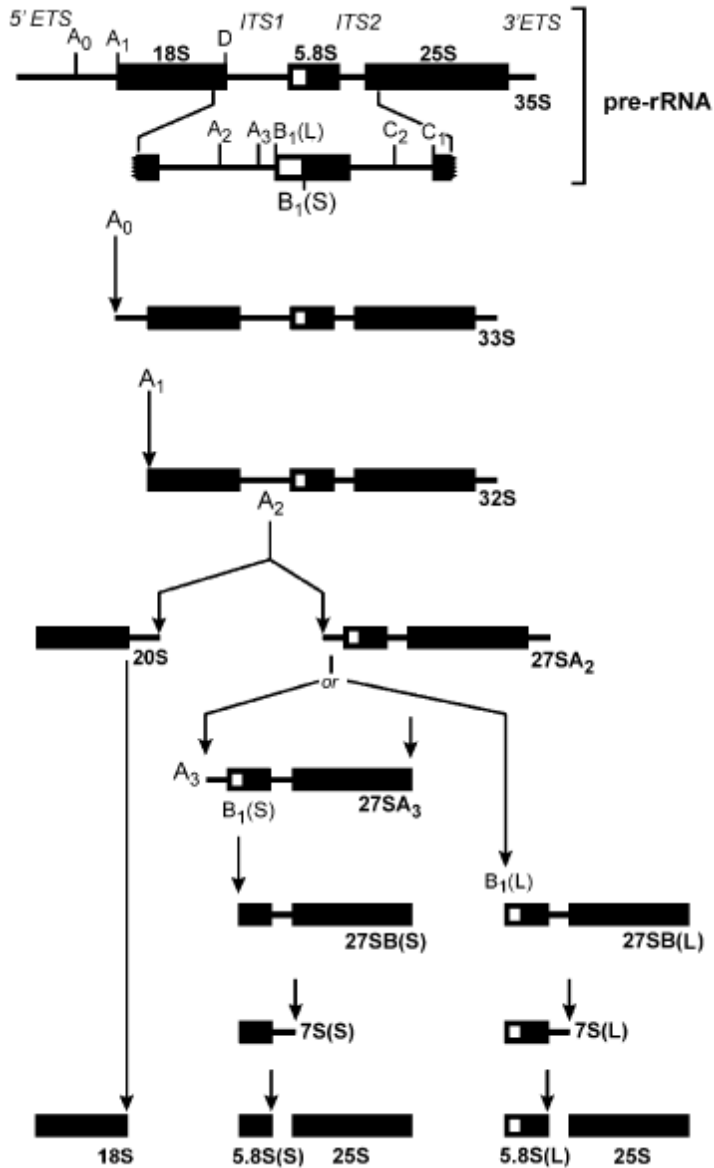


Figure 6: Pre-rRNA Processing During Ribosome Biogenesis

Sequential cleavages are shown and sites of cleavage are specified. Figure Credit: (Banneman & Baserga, 2004)¹⁴

While precursor rRNAs are being processed into mature rRNAs, ribosomal protein genes are transcribed by RNA Pol II in the nucleus, and the mature mRNAs are transported to the cytoplasm where the ribosomal proteins are synthesized. Most of these proteins are then transported back to the nucleus and/or nucleolus where they are incorporated into nascent ribosomes in coordination with 35S rRNA processing. The 90S pre-ribosome is the first well-defined intermediate in this process. As outlined in Figure 7, a variety of cleavages and factor-assisted ribosomal protein association processes occur, ultimately forming pre-small and large subunits (43S and 66S, respectively). Within the 90S pre-ribosome, the pre-rRNA is cleaved at either site A_0 or A_3 yielding the $90SA_0$ and $90SA_3$, respectively. The $90SA_3$ complex primarily contains factors necessary for 40S maturation while factors needed for 60S maturation associate later. The $90SA_0$ complex is cleaved at sites A_1 and A_2 yielding the 43S and 66S particles, respectively.¹⁵ After transportation from the nucleolar sub-compartment to the nucleus and a variety of additional ribosomal protein associations, mature 40S and 60S subunits are formed.

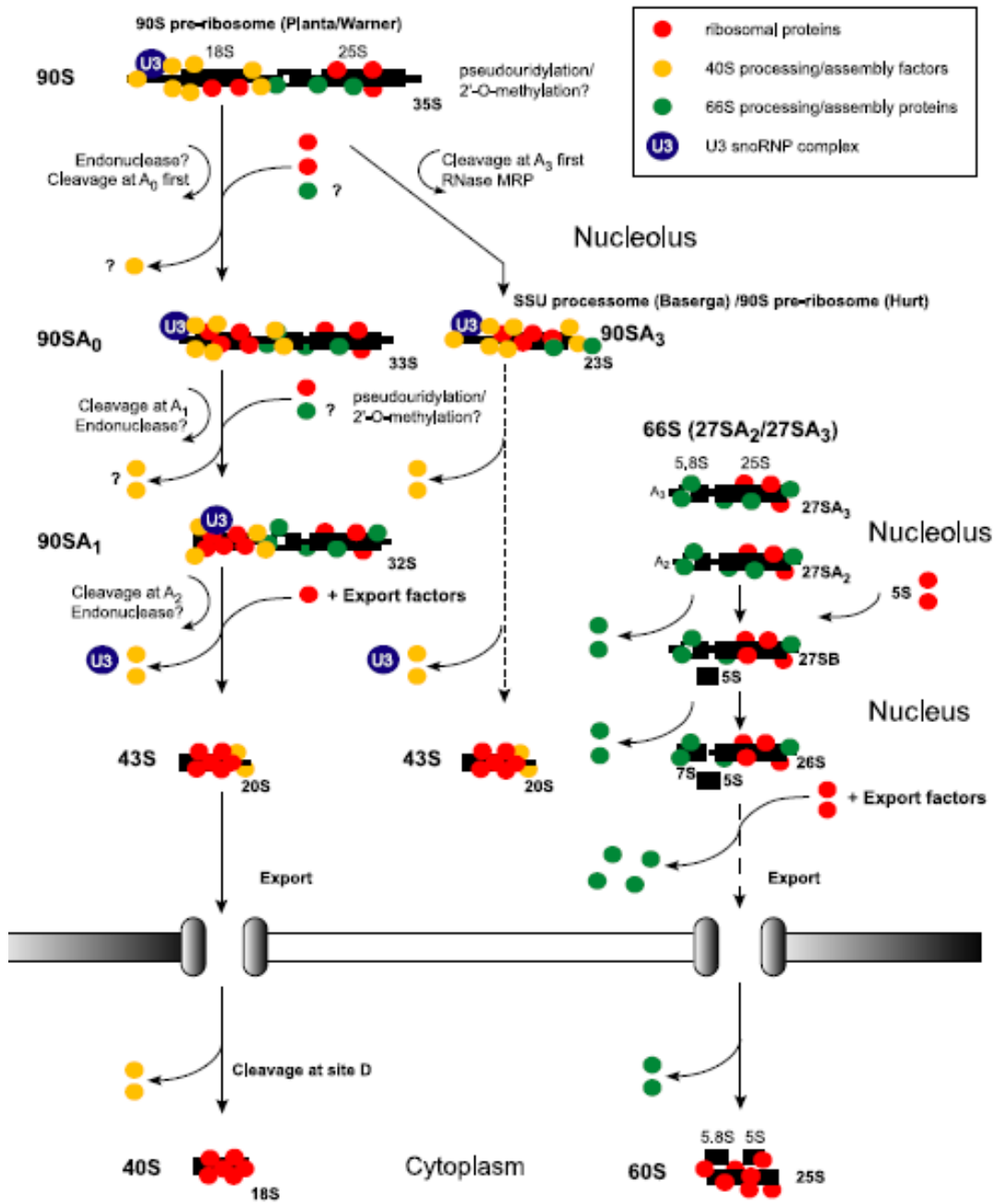


Figure 7: Model of Ribosomal Subunit Assembly

Flowchart of approximate assembly of ribosomal proteins into subunits. Figure credit: (Granneman & Baserga, 2004)¹⁴

Eukaryotic Translation

Once fully assembled, functional ribosomes are able to engage in their primary function – translation. The process of protein translation can be broken down into four well-orchestrated steps: initiation, elongation, termination, and recycling.

Initiation. The overall process of translation initiation begins with recruitment of the small subunit and initiator tRNA to the mRNA, and ends with the binding of a methionyl initiator tRNA (Met-tRNA_i) to an AUG start codon. The process is highly ordered and regulated. The translation of most eukaryotic mRNAs is initiated via a scanning mechanism.^{16–18} The small subunit is preloaded with Met-tRNA_i complexed with eIF2 and GTP. Eukaryotic initiation factors eIF1, eIF1A, eIF3, and eIF5 assist with loading this ternary complex onto the small subunit. These factors also bind directly to the 40S subunit in a cooperative manner. The 40S subunit and all of its associated factors assemble into what is known as the 43S pre-initiation complex (43S PIC), and the entire body then attaches to the mRNA. Binding of the 43S PIC to the mRNA is assisted by eIF4F, -4A, -4B, and poly(A)-binding protein (PABP). The 5' untranslated region (UTR) is then inspected, base by base and triplet by triplet, until an AUG start codon is located.^{18,19}

While an AUG codon is necessary for initiation, it is not sufficient. The initiator AUG must be in “optimal sequence context”^{17,20,21} In addition to being located in the 5' UTR of an mRNA, the presence of a purine in the position 3 bases upstream of an AUG makes an AUG more likely to participate in initiation, even if another AUG is located upstream. This is the basis for a process termed “leaky scanning”, in which upstream

AUG codons in poor sequence contexts may be bypassed for a more downstream AUG in better sequence context.^{17,20}

Base pairing of Met-tRNA_i with the start codon stimulates hydrolysis of the GTP bound to eIF2, stimulating release of eIF2-GDP along with the remaining eIFs except eIF1A. 60S subunit joining is stimulated by eIF5B-GTP. GTP hydrolysis upon subunit joining promotes the dissociation of eIF5B-GDP along with eIF1A. eIF2B, a guanine nucleotide exchange factor (GEF), recycles eIF2-GDP back to eIF2-GTP to prepare it for a new round of initiation. At the conclusion of the initiation process, the result is an 80S ribosome with Met-tRNA_i in the peptidyl site (P-site) positioned over the AUG start codon.

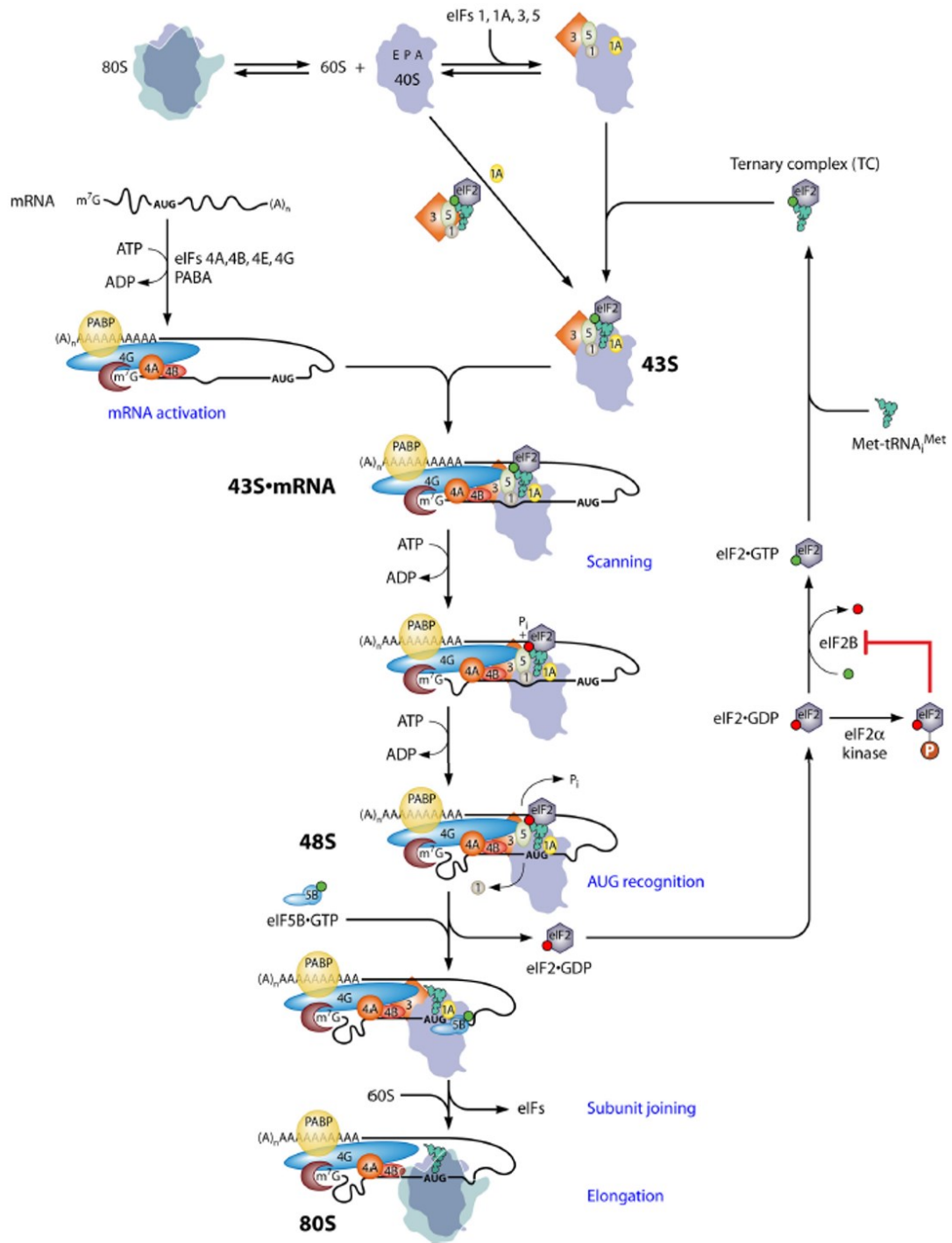


Figure 8: Overall Process of Canonical Eukaryotic Translation Initiation

Image from Hinnebusch¹⁸

Elongation. Elongation is the multistep cycle that results in addition of amino acids to the growing polypeptide chain. It begins where initiation ends; the 80S ribosome is positioned on the mRNA transcript with Met-tRNA_i in the P-site and both the A- and E-sites are empty.²² The second codon of the ORF rests in the A-site awaiting a cognate aminoacylated tRNA (aatRNA).

In a process parallel to protein synthesis, tRNAs are charged with amino acids by aminoacyl tRNA synthetases in a process called aminoacylation. This class of enzymes couples hydrolysis of ATP with binding of specific amino acids to their designated tRNAs. Once charged, tRNAs are rendered competent for ribosome binding.

The first step of the elongation process is aa-tRNA selection and accommodation. Aminoacyl-tRNAs are delivered in a ternary complex with eEF1A (the prokaryotic homolog is EF-Tu) and GTP to the “A/T site” of the ribosome. The anticodon stem loop of the tRNA samples the A-site codon while the rest of the tRNA, adopting a distorted conformation, occupies the “T-site”. The distortion is an energetically unfavorable conformational change, but the thermodynamic stability of a perfect codon-anti codon pairing offsets that energy increase.²²

Initial binding of all tRNAs sampling the A-site codon is rapid and non-specific. That is, the rates of initial binding for cognate, near-cognate, and non-cognate tRNAs are the same, giving all tRNAs an equal opportunity to bind initially. Selection for cognate aa-tRNA is due to stabilization of the anticodon stem loop (ASL) of the incoming tRNA in the A-site by base-pairing interactions. At this stage, the degree of base pairing between the codon and anti-codon leads to discrimination of non-cognate tRNAs. Following codon recognition, 18S rRNA bases A1755, A1756 (helix 44), and G577

(helix 18) flip out and interact with the first two codon-anticodon base pairs and stabilizing the tRNA in the A-site.^{8,23} A study on *Thermus thermophilus* ribosomes indicated that A1493 (A1756 in eukaryotes) binds in the minor groove of the first codon-anticodon pairing while A1492 (A1755 in eukaryotes) and G530 (G577) interact with the minor groove of the second base pair.²⁴ Formation of these and other small-scale interactions in the large subunit, small subunit, and EF-Tu (eIF1A) activate the elongation factor's GTPase function. This stabilization and GTPase activation does not occur when non-cognate tRNAs bind. As a consequence, this is the first proofreading step in the elongation process.

The tRNA stabilization signals the GTPase associated center of the LSU and triggers the hydrolysis of GTP with the help of ribosomal protein uS12 (previously known as S13). GTP hydrolysis leads to a conformational change in eEF1A and the GDP bound form of eEF1A dissociates from the tRNA. eIF1A-induced GTP hydrolysis drives the ribosome into the rotated state. Since GTP hydrolysis occurs at a rate much slower for near-cognate tRNAs than for cognate tRNAs, GTP hydrolysis represents the second proofreading step of the elongation process^{25,26} (Table 1).

Step		Rate constant (s ⁻¹)		
		Cognate	Near-cognate	Non-cognate
Initial Binding	k ₁	110	110	60
	k ₋₁	25	25	25
Codon Recognition	k ₂	100	100	
	k ₋₂	0.2	17	
GTPase activation and GTP hydrolysis	k ₃	500	50	0.005

Table 1: Elemental rate constants of cognate, near-cognate, and non-cognate aa-tRNA binding to the A-site.

Table adapted from Rodnina, et al. 2001²⁶

After GTP hydrolysis and subsequent elongation factor and GDP release, the tRNA shifts from the hybrid A/T state to the classical A/A state (referred to as A/A because both the anticodon stem loop and the CCA end are in the A-sites of the SSU and LSU, respectively) and the ribosomal subunits assume a non-rotated conformation with respect to one another. With tRNAs now in their classical states, peptidyl transfer occurs between the α -amino group of the aa-tRNA (A-site) and the carbonyl carbon of the ester linkage of the peptidyl-tRNA (P-site). The precise mechanism of peptide bond formation is not known. Several overall mechanisms have been proposed²² but the mechanism of proton transfer in the process is still an area of contention. The rRNA elements of the PTC are highly conserved between bacteria and eukaryotes and are thought to participate in the peptide bond formation. In one model, these conserved PTC residues experience a conformational change following aa-tRNA binding. This conformational change precisely positions the peptidyl-tRNA for nucleophilic attack by the aminoacyl-tRNA.²⁷

Immediately following peptide bond formation, the tRNA in the A-site is bound to the growing polypeptide chain while the P-site tRNA has been deacylated.

Subunit rotation causes tRNAs to assume hybrid conformations (P/P and A/A to P/E and A/P, respectively).¹⁰ After peptidyl transfer, the tRNAs must each shift 3' by one codon in a process known as translocation. Binding of GTP-bound elongation factor 2 (eEF2; EF-G in prokaryotes) is thought to stabilize the rotated state of the ribosome and promote rapid GTP hydrolysis.²² Movement back to the unrotated state is driven by eEF2 induced GTP hydrolysis. The CCA end of the A-site tRNA first approaches the P-site (A/P) and upon peptide bond formation, the anticodon stem loop translocates into the P-site (P/P) leaving the A-site empty. The now deacylated tRNA is released from the E-site leaving the E-site empty as well.

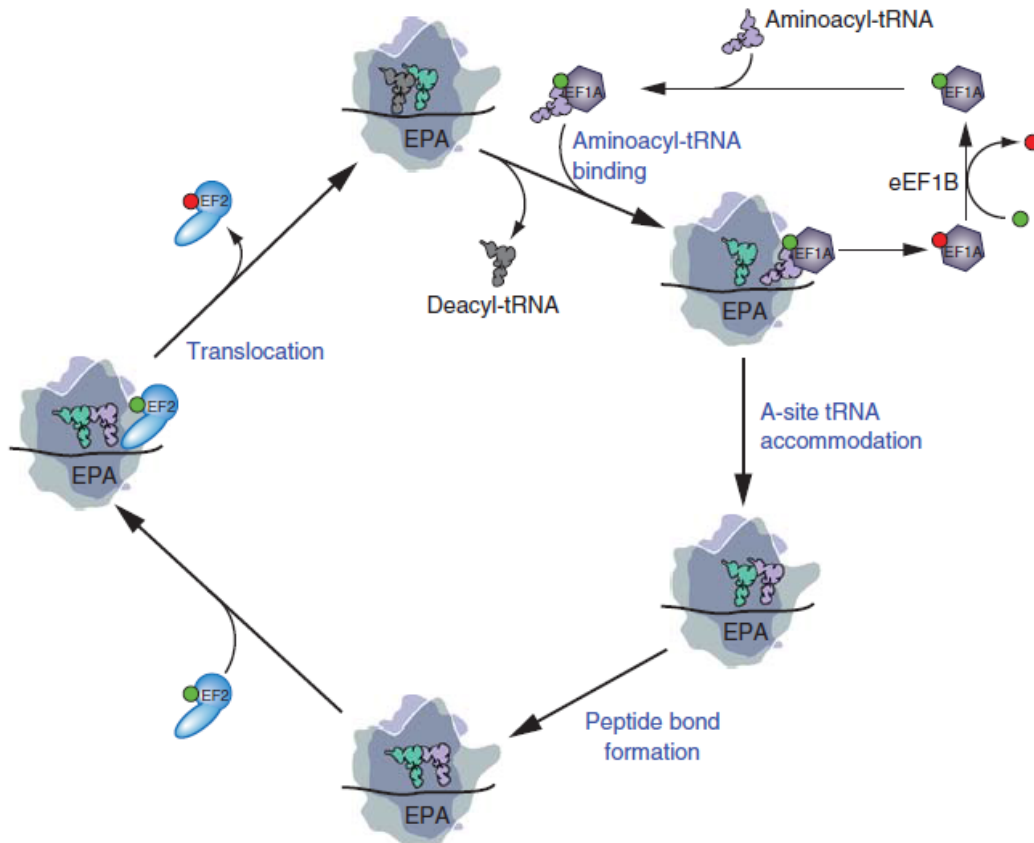


Figure 9: Model of Eukaryotic Translation Elongation Cycle.

Throughout the model, green circle indicates GTP, red circle represents GDP. Model from Dever²²

Termination and Recycling. Translation termination occurs when the ribosome reaches the end of a coding region which is signaled by a stop codon entering the A-site. In the genetic code, a stop codon is a nucleotide triplet which signals the termination of translation. Release factors are the trans-acting factors responsible for catalyzing termination. There are two classes of termination factors which have striking structural and mechanistic differences between prokaryotes and eukaryotes. In prokaryotes, class I release factors are structural mimics of tRNAs which decode stop

codons and induce peptidyl-tRNA hydrolysis. Class II release factors provide the GTPase activity necessary for peptidyl-tRNA release. There are two prokaryotic class I release factors, RF1 and RF2, which are responsible for decoding distinct stop codons (RF1 decodes UAA and UAG while RF2 recognizes UAA and UGA). There is only one prokaryotic class II release factor, RF3, which recognizes both class I factors. In eukaryotes, there are two termination factors, eukaryotic release factors 1 and 3 (eRF1 and eRF3). eRF1, the only eukaryotic class I release factor, is a structural mimic of a tRNA comprised of three structural domains. The N-terminal domain contains a highly conserved NIKS motif which has been thought to be responsible for stop codon recognition.²² The middle domain of eRF1, similar to the acceptor stem of a tRNA, extends into the PTC where it helps facilitate peptide release. Like RF1 and RF2, the middle domain of eRF1 contains a conserved Glycine-Glycine-Glutamine (GGQ motif) which is thought to be essential for catalyzing peptidyl-tRNA hydrolysis. The carboxyl terminus of eRF1 coordinates interactions with the class II factor, eRF3. eRF3 is a translational GTPase with a conserved carboxyl terminus which interacts directly with the middle domain and carboxyl terminus of eRF1. In vitro studies have shown that eRF3 both accelerates peptide release and increases efficiency of termination in a GTP hydrolysis dependent manner.²⁸

Upon stop codon recognition, the eRF1-eRF3-GTP complex binds to the ribosome in the A-site. Binding of this complex to the ribosome hydrolyzes GTP which induces repositioning of the middle domain of eRF1 in the peptidyl transferase center. This movement of eRF1 in the PTC releases GDP-bound eRF3. Prior to ribosome binding, dissociation of GTP from eRF3 is slowed by eRF1 which has been proposed to

act as a GTP dissociation inhibitor. Once the ternary complex of eRF1-eRF3-GTP binds the ribosome, this triggers the GTP hydrolysis. After eRF3-GTP release, eRF1 triggers hydrolysis of the peptidyl tRNA which releases the newly synthesized protein.

Following termination, ribosomes are removed from the mRNA and regenerated for subsequent rounds of translation in a process known as ribosome recycling. At the conclusion of translation termination, the deacylated tRNA and eRF1 bound-80S ribosome is still associated with the mRNA. Two optional outcomes are possible at this point depending on the ORF context – recycling or reinitiation. Recycling is the most common outcome of translation termination. In recycling, the first step is ABCE1-mediated dissociation of the 60S subunit leaving the deacylated tRNA-bound 40S subunit on the mRNA. This is followed by subsequent dissociation of the 40S subunit and ejection of the deacylated tRNA which is proposed to be facilitated either by canonical initiation factors or other trans-acting factors.²⁹ For reinitiation to take place, one possibility is that the recently decoded ORF is immediately upstream of another ORF which is translated without the subunits being completely recycled between the two events. Alternatively, ribosomes translating a message with only one ORF can experience incomplete recycling wherein the 40S subunit is transferred from the 3' UTR to the 5' UTR and a subsequent round of translation takes place. The mechanism of these interactions is not yet fully understood.^{22,29}

Bacterial ribosomes utilize a dedicated ribosomal recycling factor (RRF) which assists in the exit of the class I termination factor and the dissociation of the subunits. There is no eukaryotic homolog of this recycling factor and very little similarity between the termination and recycling activity between prokaryotes and eukaryotes. In

prokaryotes, RRF interacts with rotated ribosomes (which contain deacylated tRNA in the P-site) and destabilizes intersubunit bridge interactions.^{30,31} EF-G-GTP stimulates subunit dissociation and IF3 binds to the small subunit inhibiting reassociation and promoting release of the deacylated tRNA and the mRNA.

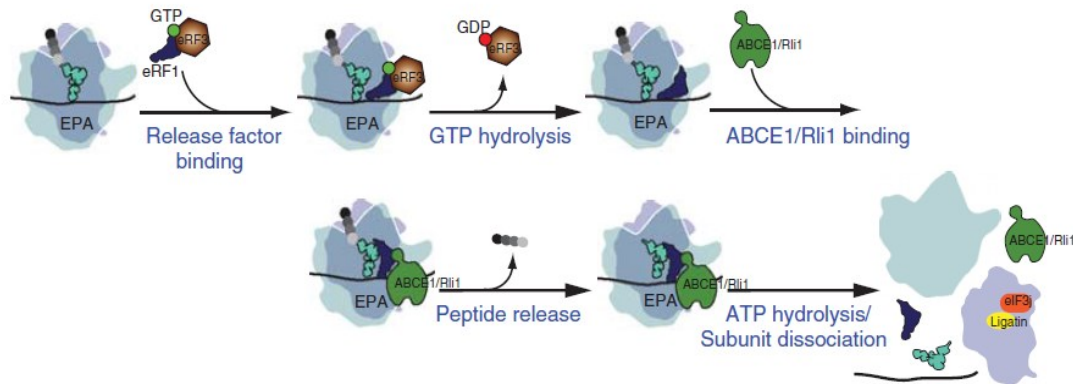


Figure 10: Eukaryotic Translation Termination and Recycling Overview

Throughout the model, green circle indicates GTP, red circle represents GDP. Model from Dever²²

Translational Recoding

The highly regulated process of translation has been well studied and described. However, canonical translation is a “rule” that, like all rules, can be broken. As such, there are a series of exceptions to the rule collectively known as translational recoding events. These recoding events, first discovered in viruses, interrupt the linear in-frame reading or canonical recognition of termination codons of an mRNA transcript.

Programmed -1 Frameshifting. The recoding event known as programmed -1 frameshifting (-1 PRF) was first discovered in the study of RNA viruses, which employ this molecular mechanism to produce appropriate ratios of structural to enzymatic

proteins. It was first discovered in the Rous Sarcoma Virus³², and has been identified in several other viruses including HIV-1, the yeast virus L-A, and SARS.^{33,34} -1 PRF signals have also been identified in several eukaryotic organisms including humans and mice.³⁵⁻³⁷ Three cis-acting RNA elements are typically required for a -1 PRF event to occur – a heptameric “slippery” sequence, a spacer region between the slippery sequence and pseudoknot, and a strong, tertiary structure (typically a pseudoknot). The form of the heptameric slippery sequence is 5'-N NNW WWH-3', in which N's represent any three identical nucleotides, W's represents three U's or A's, and H represents any nucleotide except G. The spacer region is typically 5-8 nucleotides in length and its function is to ensure proper spacing between the slippery site and pseudoknot. There are many varieties of pseudoknots, but the structure is typically a hairpin stem loop in which nucleotides from the base of the hairpin base pair with nucleotides in the loop.³⁸ In a -1 PRF event, translating ribosomes pause 5' of a strong, tertiary structure on the mRNA which is not readily resolved. The ribosome stops over the slippery site such that NNW is positioned in the P-site and WWH is positioned at the A-site. While stalled at the pseudoknot, the ribosome “slips” by one base in the 5' direction and the associated tRNAs re-associate with the mRNA in the -1 frame. Once the tertiary structure is “melted”, the ribosome continues translating in the new reading frame.

The identity of the “slippery” nucleotides and their relative degree of Watson-Crick base pairing directly affects the “slippage” of the ribosomes. A greater percentage of A/U base pairs, which are weaker than G/C base pairs, make for a “more slippery” site while the stronger G/C base pairs create a “less slippery” one. Nevertheless, the setup of the slippery sequence on the mRNA is such that a -1 PRF event results in cognate or

near-cognate codon-anticodon pairing. While paused over the slippery site, ribosomal helicases work to unwind the pseudoknot. Slippery sequences can facilitate -1 PRF events on their own, but this does not occur frequently enough to be biologically significant.³⁹ This recoding method is utilized by several viruses such as HIV-1 and the yeast virus L-A. L-A is a yeast virus which contains two partially overlapping open reading frames (ORFs) – Gag (encodes for the major coat protein) and Pol (encodes for the enzymatic protein). In order for the Gag-pol fusion protein to be produced, a programmed -1 frameshifting (-1 PRF) event must occur.⁴⁰ Changes in -1 PRF efficiency alter the Gag to Gag-Pol ratio (Figure 11) thus affecting the virus' ability to replicate.

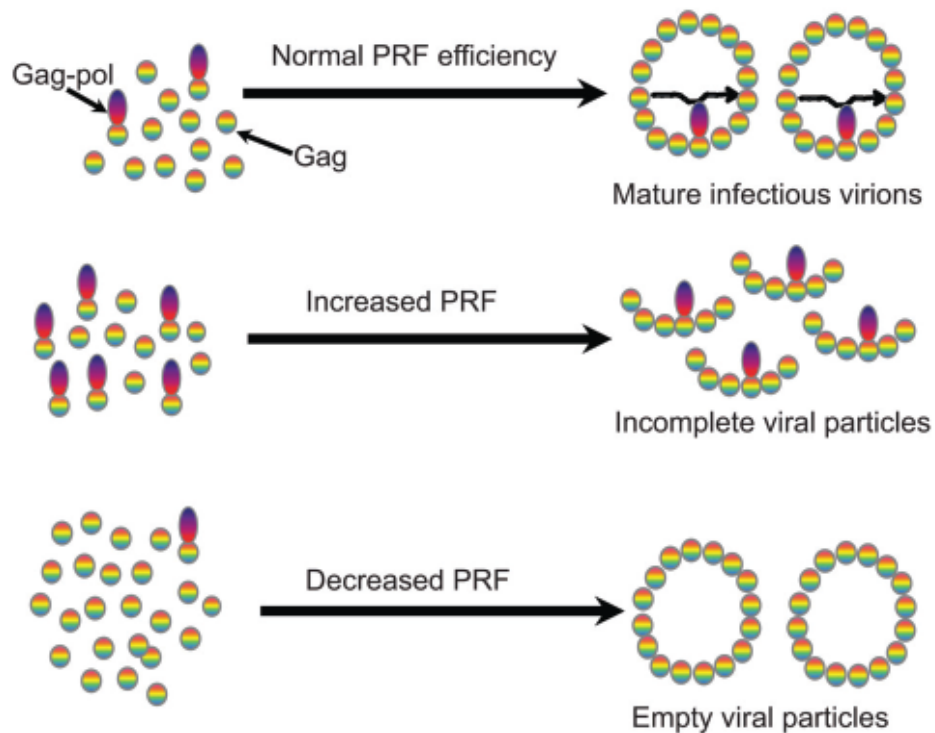


Figure 11: Programmed ribosomal frameshifting in viruses.

Changes in -1 PRF efficiency alter the Gag-pol ratio which affects viral particle assembly. Image credit: Dinman, et al (2012)⁴¹

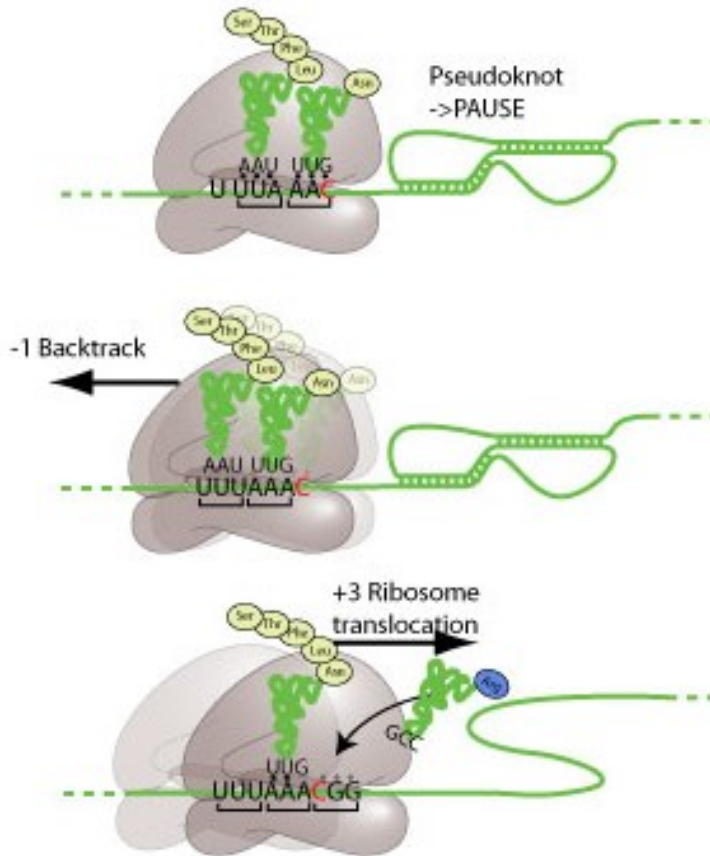


Figure 12: General Mechanism for -1 PRF

Green represents RNA molecules – Translating ribosome pauses at pseudoknot and slips back by one base altering the reading frame. Image credit: viralzone.expasy.org

Programmed +1 Frameshifting. In a programmed +1 ribosomal frameshift (+1 PRF) event, the translational reading frame is shifted by one nucleotide in the 3' direction. +1 PRF events are employed most notably by transposable elements.⁴²⁻⁴⁴ +1 PRF signals tend to be unique. The best characterized +1 PRF system is the Ty1 yeast retrotransposable element which consists of a 7-nucleotide slippery site, a near-cognate peptidyl tRNA in the P-site, and an empty A-site with a “hungry” A-site codon.⁴² Similar

to previously described L-A, *TyI* consists of gag and pol overlapping ORFs. In the absence of a +1 PRF event, only gag will be translated. The +1 PRF event is necessary for the translation of gag-pol fusion protein. A near cognate tRNA in the P-site has been found to be critical for a +1 PRF event.⁴² During a +1 PRF event, a near-cognate tRNA occupies the *TyI* slippery site (5'-CUU AGG C-3'). That is, rather than a cognate aa-tRNA^{Leu}_{AAG}, the near cognate aa-tRNA^{Leu}_{UAG} is present. This results in weaker base pairing which is more easily broken during the frameshifting event. The A-site codon, AGG, codes for arginine. However, due to the low abundance of the appropriate complimentary tRNA, stalling occurs. While stalled, the ribosome can slip forward by one base and the P-site tRNA re-associates with the mRNA in the +1 frame. Now with a more abundant mRNA codon in the A-site (a glycine GCC tRNA, in the case of *TyI*), a cognate tRNA rapidly binds to the A-site and translation continues.

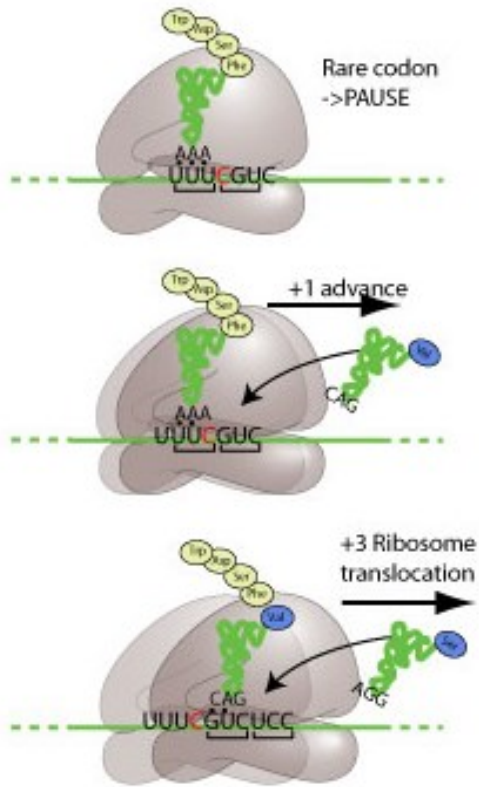


Figure 13: Example of a +1 PRF Mechanism.

There are several putative mechanisms for +1 PRF. This is the mechanism utilized by the Ty1 retrotransposon, but other mechanisms of +1 PRF exist which have yet to be explored. Image credit: viralzone.expasy.org

Missense and Nonsense Codon Suppression. In order to synthesize proteins at a rate of ~10-20 amino acids per second, the process of translation must predominantly remain accurate and free of errors. Suppression of missense and nonsense codons are two events which occur as a result of reduced translational accuracy (fidelity). Missense events occur as a result of near- or non-cognate tRNA mistakenly accommodating in the A-site. When a translating ribosome is able to bypass a stop codon by instead

incorporating an amino acid into the growing polypeptide chain, this phenomenon is known as nonsense codon suppression. Nonsense codon suppression can occur in a programmed or non-programmed manner. Programmed nonsense codon suppression is the primary mechanism of selenocysteine incorporation into proteins and is the result of communication between cis-acting elements on the mRNA.^{45,46}

Small Molecule Translation Inhibitors

Antibiotics are compounds which selectively kill or inhibit the growth of microorganisms. Many antibiotics are translation inhibitors and their binding sites are located in the peptidyl transferase center (PTC) of the ribosome. The PTC of the LSU contains two hydrophobic crevices which are thought to play an important role in the ribosomes interaction with antibiotics. Antibiotic assays can provide an informative, qualitative probe of translational fidelity and have been utilized for the research presented in this thesis.

Two antibiotics involved in this study, anisomycin and paromomycin, are both translation inhibitors. Anisomycin has attracted interest in recent years in the context of chemotherapy, but due to a lack of species specificity, is not utilized in the treatment of human infections.⁴⁷ It has been described as a structural analog of puromycin, another translation inhibitor. Anisomycin has a p-methoxybenzene moiety which inserts itself into the A-site cleft of the large subunit. The A-site cleft, one of two aforementioned hydrophobic crevices in the PTC, is formed by A2486 and C2487 and the top of the base pair between A2488 and U2535 (*Haloarcula marismortui* numbering). The p-methoxyphenyl moiety stacks onto C2487, thus stabilizing the drug in the A-site. This crevice forms the part of the A-site which contacts amino acid side chains of A-site

substrates. Anisomycin, therefore, competitively inhibits binding of tRNAs in the A-site. Paromomycin is an aminoglycoside which binds to critical bases in the decoding center causing conformational change.⁴⁷ These bases, A1492 (A1755 in eukaryotes), A1493 (A1756 in eukaryotes) and G530 (G577) normally flip out to form A-minor interactions with the codon-anticodon minihelix upon cognate tRNA binding in the A-site. These interactions are critical for translational fidelity as they are only formed when a cognate codon-anticodon pair is formed. With these critical bases occupied by paromomycin, misincorporation rates increase.⁴⁷ Due to the nature of these ribosome-drug interactions, these antibiotics and others have been used in ribosome studies as a qualitative probe of PTC and DC function as well as translational fidelity.

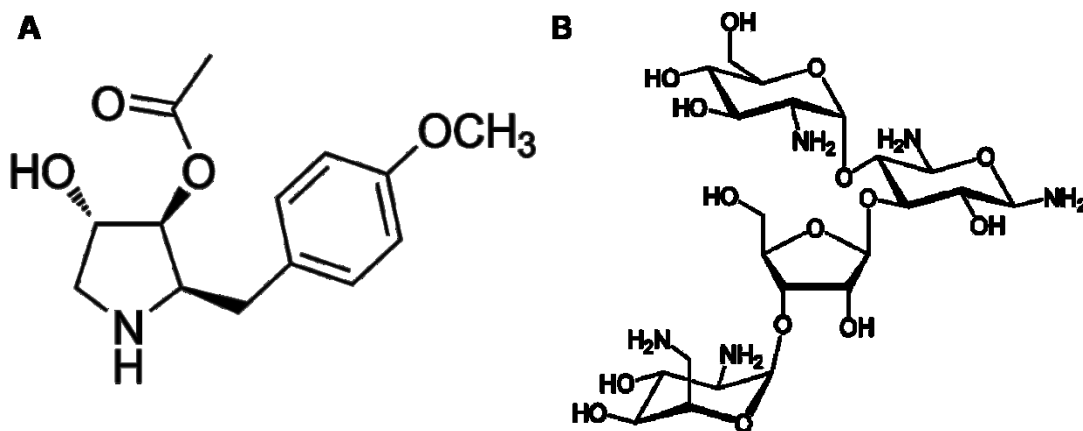


Figure 14: Structures of Anisomycin & Paromomycin.

(A) Anisomycin and (B) Paromomycin

Ribosomal Proteins uS19 and uS13

In bacteria, ribosomal protein uS13 (previously known as S13 in prokaryotes and S18 in eukaryotes) participates in two intersubunit bridges – B1a and B1b/c. However, in eukaryotes, uS13 participates in the B1b/c bridge and a neighboring protein, uS19

(previously S19 in prokaryotes and S15 in eukaryotes), is the SSU side of bridge B1a. Eukaryotic ribosomal protein uS13 consists of two distal functional domains, one which is involved in 16S rRNA recognition and the other which interacts tightly with uS19 forming a dimer between the two proteins.⁴⁸ In one study, these functional domains were separated *in vitro* yet still maintained the capacity to bind their respective partners.⁴⁹

The location of these proteins makes them fitting candidates for further study. Both proteins are located in the head region of the SSU which undergoes large-scale rearrangements during translation. Additionally, both proteins have extensions which are known to interact with the decoding center. In human ribosomes, a ten-amino acid fragment of uS19 in the C-terminal crosslinks with the A-site mRNA codon.⁵⁰ The position or existence of the cross-linking on uS19 did not depend on the nature of the A-site bound codon suggesting that uS19 is always present in the A-site independent of tRNA binding.⁵⁰ One study indicated that prokaryotic uS13 interacts with P-site bound tRNA through its extended C-terminus.⁵¹



Figure 15: Location of uS13 and uS19 in the 80S Ribosome & 40S Subunit

(A) uS13 (yellow) and uS19 (hot pink) and their respective intersubunit bridge partners uL5 (cyan) and LSU H38 (red). (B) Location of uS13 and uS19 in the head region of the SSU. Image created in PyMol from Yusupov, et al (2011)¹²

Both proteins are involved in intersubunit bridge interactions with LSU partners which been extensively studied. The LSU side of the B1a bridge, Helix 38 (aka the A-site finger) is known to contact the D-loop of aminoacyl tRNA (aa-tRNA).⁵² Reverse genetics studies of Helix 38 suggest that the B1a bridge plays a role in aa-tRNA selection. Pharmacogenetic and biochemical data in this study agreed as B1a mutants of H38 conferred resistance to antibiotics which block aa-tRNA binding and the mutants showed increased affinity for aa-tRNA. H38 contains an arc of unpaired “hinge bases” which provide flexibility to the network of otherwise rigid helices in the large subunit. Finally, this helix was also suggested to be part of the information exchange network between several functional centers of the ribosome including the peptidyl-transferase center (PTC) and GTPase associated center.⁵²⁰ Bridge B1b/c mutants of uL5 (previously known as L11) have been shown to confer long-range changes in rRNA structure.⁴ A reverse genetics study of L11 revealed an extensive network of information flow between distal regions of the ribosome in the large and small subunits. Also, the L11 P-site loop helps to optimize ribosome function by monitoring P-site occupancy. The P-site loop is flexible and extends into the P-site when the binding pocket is unoccupied, and retracts into a terminal loop of Helix 84 of the 25S rRNA when a peptidyl tRNA occupies the P-site.

Both uS13 and uS19 have been implicated in ribosome biogenesis. Depletion studies have indicated that before pre-40S particles can be exported from the nucleus for final processing during biogenesis, uS19 must be associated with them. Rps15p-depleted cells experience decreased synthesis of 18S rRNA as well as retention of 20S pre-RNA in the nucleus.⁴⁸ In yeast, uS13 was shown to be nonessential for cell growth, but necessary

during ribosome biogenesis for processing of 35S pre-rRNA at the A₂ site.⁴⁸ *E. coli* studies of the prokaryotic homolog of uS13 (previously known as S13) suggest that, during biogenesis, uS13 assembles into ribosomes along with neighboring proteins as part of the S7 assembly branch. However, unlike neighboring proteins, uS13 assembly into pre-40S particles does not occur in the presence of S20, a ribosomal protein more than 100 Å away.⁵³

Research Overview

The research presented in this thesis began with a structure and function study of ribosomal protein uS19. As mentioned, both uS13 and uS19 are located in the head domain which, during translation, experiences the largest rearrangements of any SSU domain. Additionally, the C-terminal domain of uS19 approaches the A-site codon suggesting a potential link between uS19 and A-site function. Several details suggest a cooperative role for these two proteins. One of the functional domains of uS13 interacts tightly with uS19 forming a dimer interface between the two proteins. That uS13 in prokaryotes participates in two intersubunit bridges, but shares one of these bridges with uS19 in eukaryotes is intriguing. The split suggests an evolutionary advantage for the downsizing of uS13 which is worth exploring further.

Chapter 2 specifically addresses the role of the uS19-uS13 interaction in the yeast *Saccharomyces cerevisiae* in translational fidelity and ribosomal rotational equilibrium. Chapter 3 is an overview of the materials and methods necessary for the study. Chapter 4 is a discussion of the conclusions drawn from this study.

Chapter 2: Ribosomal Protein uS19 (S15)

Introduction

Conversion of the genetic information encoded in mRNAs into proteins is carried out by large ribonucleoprotein particles called ribosomes. Yeast ribosomes are 3.6 kDa structures composed of 79 ribosomal proteins and 4 ribosomal RNA molecules. The two ribosomal subunits contain their own functional centers responsible for carrying out separate functions. The small subunit (SSU) directs the bulk of translational initiation, and contains the messenger RNA (mRNA) decoding center. The large subunit (LSU) harbors several functional centers, most notably the peptidyltransferase center (PTC) which is the catalytic site of polypeptide synthesis, three tRNA binding pockets, and the GTPase associated center. During the elongation stage of translation, the large and small subunits work in concert. With each cycle of amino acid incorporation into the nascent polypeptide chain, the two subunits rotate with respect to one another by ~ 8 Å.^{9,10,54} Ribosomes at the two extreme stages this process are known as rotated and non-rotated.⁵⁵

In translating ribosomes, the two subunits are connected by highly conserved interactions known as intersubunit bridges. The roles of these bridges include providing structural stability and transmitting information between distal functional centers of the ribosome.^{4,12} While some bridges remain intact throughout the translation elongation cycle, others break and re-form. Previous studies have shown that ribosomal rotational status can be monitored by monitoring this dynamic process as the ribosome transitions between the rotated and non-rotated states.^{31,54,56,57} In particular the solvent accessibility of the B7a bases G577 and A1577 have been exploited as indicators of ribosome

rotational status.^{56,57} The core intersubunit bridges are highly conserved in all domains of life. In particular, the B1 family of bridges (divided into B1a and B1b/c) link the head of the SSU with the central protuberance of the LSU; these structures undergo the largest degree of intersubunit rotation during the elongation cycle.^{11,58} While these bridges are highly conserved, the identities of the interacting partners differ between prokaryotes and archaea compared to eukaryotes. In the prokaryotes and archaea, a single SSU protein, uS13, partners with H38 (the A-site finger) and uL5 to form the B1a and B1b/c bridges respectively. In eukaryotes, it appears that the SSU component was split into two separate proteins during the course of evolution. One of these, also known as uS13, only participates in bridge B1b/c with uL5 in eukaryotes. The other, called uS19 (previously known as S15) is the SSU partner in the B1a bridge with H38. High resolution crystal structures of yeast ribosomes reveal that the two proteins interact extensively with one another.¹²

In addition to its role as the SSU half of the B1a intersubunit bridge, the 142 amino acid eukaryotic uS19 also plays an integral role in small subunit biogenesis: while depletion of uS19 permits exit of 20S pre-rRNA molecules from the nucleolus, they are retained in the nucleus, demonstrating that assembly of uS19 into SSU precursors is required to render 43S particles competent for export from the nucleus to the cytoplasm.⁴⁸ In mature ribosomes, crosslinking studies show that the unstructured C-terminal tail of eukaryotic uS19 reaches the ribosomal decoding center.⁵⁰ Its LSU partner, H38 is a large structure that interacts with numerous functional centers in the LSU including the D-loop of aminoacyl tRNA (aa-tRNA), the peptidyltransferase center (PTC) and GTPase associated center.⁵² During translation elongation, the B1a bridge is

intact when ribosomes are in the unrotated state. However, when ribosomes become fully rotated, H38 and uS19 separate by 10 Å breaking the B1a bridge. Eukaryotic ribosomal protein uS13 (previously S18) is a 17 kDA protein and the small subunit side of the B1b/c bridge in eukaryotes. In yeast, uS13 is encoded by two paralogous genes, *RPS18A* and *RPS18B* which are identical with the exception of silent mutations in their DNA sequences. Several studies have been performed in bacteria which suggest that prokaryotic uS13 plays an important role in ribosome function.^{49,51,53,59,60} In one study, the gene encoding *E. coli* uS13, *rpsM*, was deleted and mutants showed subunit joining defects as well as decreased translation initiation.⁵¹ *E. coli* uS13 was also shown to be essential for maintaining the pretranslocation state during translation.⁵³ During yeast ribosome biogenesis, uS13 is required for processing of 35S pre-rRNA at the A₂ site.⁴⁸ In mature ribosomes, uS13 interacts with uL5 to form the B1b/c intersubunit bridge. While this bridge remains intact through ribosome rotation, the specific interactions between the two proteins change.

uS19 and uS13 have been indirectly implicated in transmitting information between functional centers on the two subunits. For example, reverse genetics studies of H38 suggested that information pertaining to aa-tRNA selection in the SSU decoding center is transmitted from uS19 across the B1a intersubunit bridge to H38, from which it is distributed to functional centers in the LSU.⁵² Similarly, analyses of uL5 mutants identified a network of allosteric information exchange spanning the length of the LSU tRNA binding cleft, through uL5, across the B1b/c bridge to the decoding center, presumably through uS19 and uS13.^{4,61} While uS13 and uS19 are distinct proteins, they physically interact with one another and thus structurally mimic the single prokaryotic

uS13^{12,48}. Thus, while split, the two proteins remain intimately connected, begging the question of why such a division was selected for by the evolutionary process. The current study employed a series of mutants lying in the uS13/uS19 interface to address this issue. We find that residues L₁₁₂-H₁₁₄ on the uS13/uS19 interface acts as a ball-and-socket joint conferring greater flexibility to the head region of eukaryotic ribosomes. Interface mutants were found to shift ribosomal rotational equilibrium toward the unrotated state and exhibited decreased affinity for the translocase eukaryotic elongation factor 2 (eEF2) and increased affinity for elongation ternary complex. We suggest that the evolutionary addition of several eukaryote-specific structural elements has led to more complex ribosomes which benefit from a greater amount of structural flexibility.

Results

Mutant viability screen reveals inviable uS19-uS13 interface mutants

Using available cryo-EM⁶² and x-ray crystal¹² structures of yeast ribosomes as a guide, a region of 19 residues of uS19 was identified as potentially interacting with uS13 in yeast ribosomes. Initially, three stretches of six or seven amino acids in this region were mutated to alanine (Table 2). Site-directed mutagenesis was employed to synthesize the mutants. Mutant plasmids were separately transformed into a *ARPS15* yeast strain. All three mutants were inviable as the sole form of uS19. Eight additional mutants were synthesized with stretches of two or three alanines (Figure 16). Of the eight new mutant strains produced, only one (EM110-111AA) was inviable.

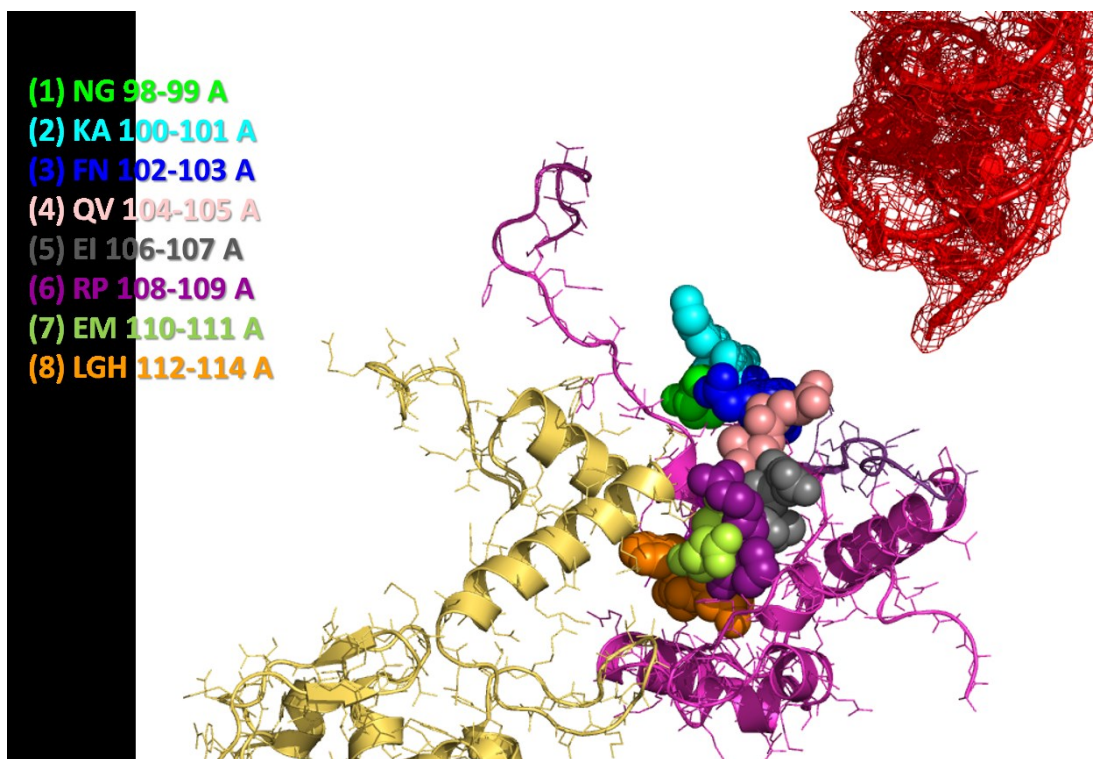


Figure 16: Locations of uS19-uS13 Interface Mutants.

Mutants on uS19 (hot pink) in the region which interfaces with uS13 (yellow). LSU H38 is in red. Image created in PyMol from Yusupov, et al (2011)¹²

Original Mutants	Smaller Stretch Mutants		
NGKAFN 98-103 A*	NG 98-99 A	KA 100-101 A	FN 102-103 A
QVEIRP 104-108 A*	QV 104-105 A	EI 106-107 A	
EMLGH 109-114 A*	RP 108-109 A	EM 110-111 A*	LGH 112-114 A

Table 2: Summary of uS19-uS13 Interface Mutants Generated. Asterisk denotes inviable mutant.

LGH112-114 mutant exhibits pronounced temperature and drug sensitivity

Mutants were assayed using standard 10-fold dilution spot assays at low temperature (20°C), optimal temperature for yeast growth (30°C), and high temperature (37°C). At 30°C, all mutants exhibited a growth rate comparable to wild-type except LGH112-114AAA which exhibited slow growth.(Figure 17A) EI106-107AA exhibits a slow growth phenotype at 37°C while LGH112-114AAA is not viable at 37°C. Sensitivity to two small molecule translation inhibitors was also assayed using dilution spots. While all other mutants exhibited growth rates comparable to wild-type in the presence of anisomycin and paromomycin, LGH112-114AAA was sensitive to both drugs (Figure 17C).

The yeast L-A or “killer” virus assay was utilized as a preliminary qualitative screen for translational fidelity. Killer is composed of the L-A helper and M₁ satellite viruses. L-A is a 4.6 kb double-stranded RNA yeast virus which contains two partially overlapping open reading frames (ORFs) – Gag (encodes for the major coat protein) and Pol (encodes for the enzymatic protein). In order for the Gag-pol fusion protein to be produced, a programmed -1 frameshifting (-1 PRF) event must occur. Changes in -1 PRF efficiency affect the Gag to Gag-Pol ratio, inhibiting the ability of cells to maintain M₁.⁴⁰ Killer virus gets its name from its killer phenotype. K⁺ cells, those infected with Killer virus, secrete a toxin which kills K⁻ cells, forming a zone of growth inhibition around the patch of K⁻ cells. This toxin is encoded by M₁. Cells expressing wild-type *RPS15* maintained the killer phenotype as evidenced by the ring of growth inhibition surrounding the patch of wild-type cells (Figure 17B). Most mutants also exhibited K⁺

phenotype. In contrast, mutant strains NG98-99AA and LGH112-114AAA exhibited K⁻ phenotype indicative of a translational fidelity defect.

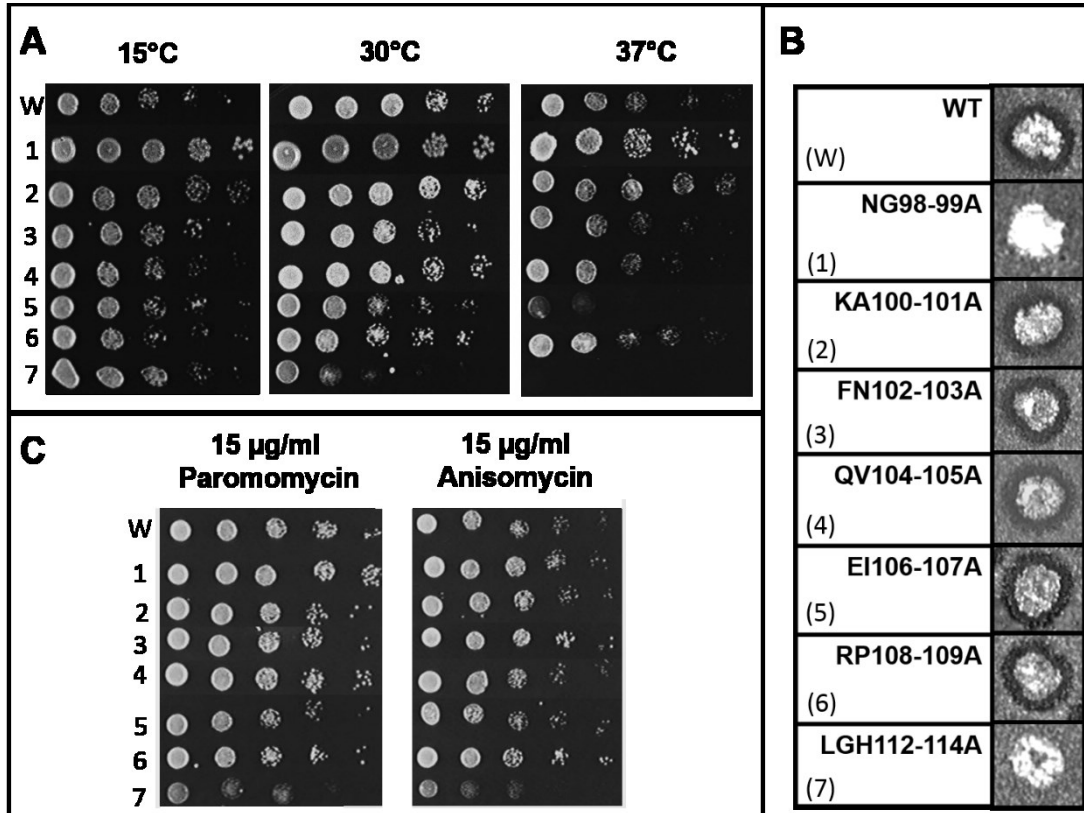
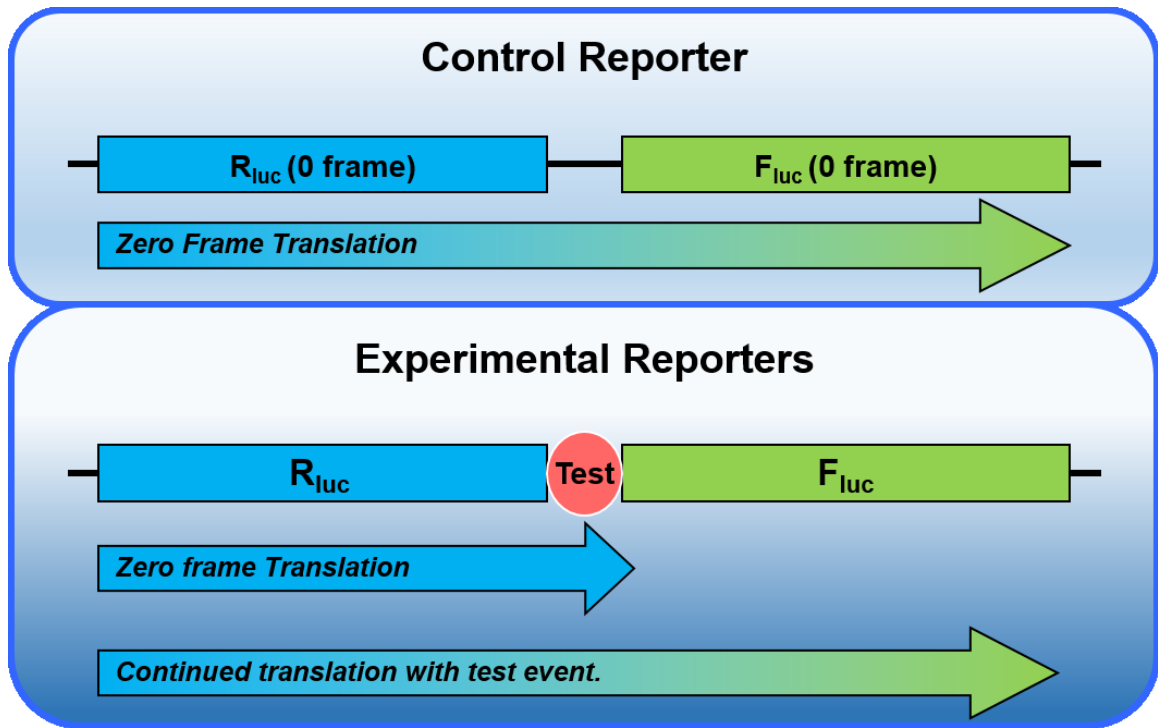


Figure 17: Genetic Analyses

Ten-fold serial dilution spot assays for (A) temperature sensitivity and (C) sensitivity to 15 µg/ml of the small molecule translation inhibitors paromomycin and anisomycin. (B) Killer maintenance assay was performed as a qualitative measure of translational fidelity.

uS19-uS13 interface mutations alter translational fidelity

As a quantitative measure of translational fidelity, bicistronic luminescence reporter assays were employed. The four reporter plasmids used assay for +1 PRF, -1 PRF, suppression of nonsense codons, and suppression of missense codons. Mutant strains were transformed separately with each of the four test constructs as well as the readthrough control construct (Figure 18) and percentage of frameshifting was determined. NG98-99AA & EI106-107AA exhibited -1 PRF rates roughly 1.5-fold higher than WT. (Figure 19) EI106-107AA also conferred increased rates of nonsense codon suppression. (Figure 20) LGH112-114AAA exhibited a +1 PRF rate 1.5-fold higher than WT (Figure 19).



$$\text{Fidelity} = \frac{(\text{Fluc}_{\text{test}}/\text{Rluc}_{\text{test}})_{\text{exp}}}{(\text{Fluc}_0/\text{Rluc}_0)_{\text{control}}} \times 100\%$$

Figure 18: Frameshifting Assay Design

(**Top**) Readthrough control construct consists of both renilla and firefly luciferase ORFs in the zero-frame with respect to one another. (**Middle**) Test constructs consist of test signal between constructs and firefly luciferase in appropriate frame depending on the signal (ie. Firefly in -1 frame if the signal is a -1 PRF). (**Bottom**) Percent frameshifting calculated as a ratio of ratios. Image credit: Dr. Jonathan Dinman

LGH112-114AAA and QV104-105AA conferred opposing effects on near-cognate missense codon suppression. Mutant LGH112-114AAA exhibited a 5-fold increased rate of missense codon suppression while QV104-105AA exhibited a 2-fold decrease. Based on these findings, QV104-105AA and LGH112-114AAA were selected for further study, primarily based on their opposing effects on missense codon suppression.

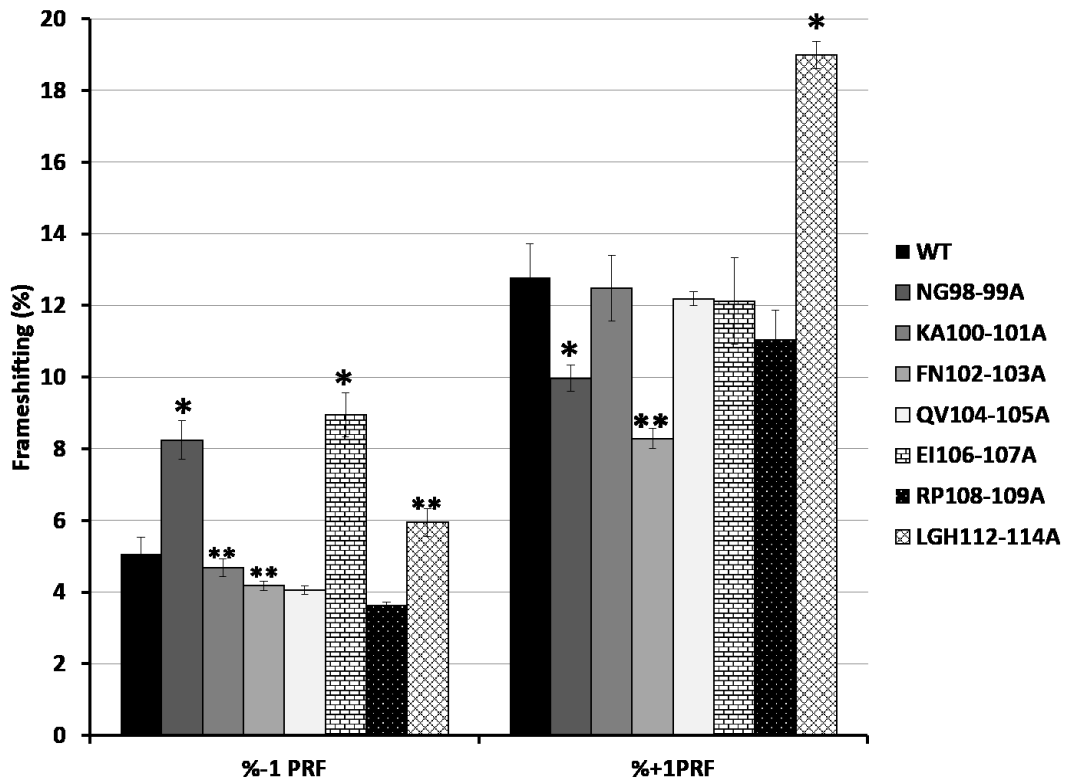


Figure 19: uS13/uS19 mutants exhibit varying effects on -1 and +1 Programmed Ribosomal Frameshifting

Yeast cells expressing either wild-type or mutant forms of uS19 were transformed with dual luciferase reporter and readthrough control plasmids and rates of translational recoding were determined. Error bars denote standard error. * $P < 0.05$, ** $P < 0.01$ comparing *WT* to mutants

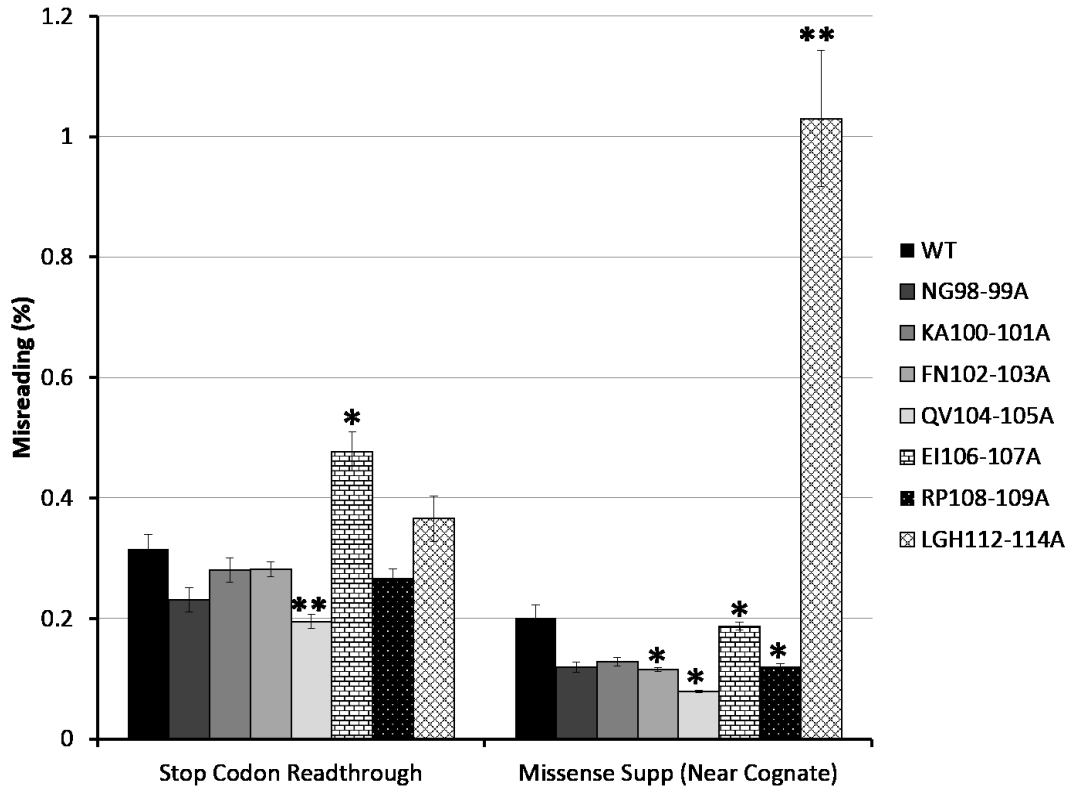


Figure 20: LGH112-114AAA and QV104-105AA exhibit opposing effects on missense codon suppression

Yeast cells expressing either wild-type or mutant forms of uS19 were transformed with dual luciferase reporter and readthrough control plasmids and rates of translational recoding were determined. Nonsense codon suppression construct consists of an in-frame stop codon between the two ORFs. Missense suppression rates were determined by incorporation of cognate arginine (AGA) in place of near cognate serine (AGC) at position 248 in the firefly ORF. Error bars denote standard error. * $P < 0.05$, ** $P < 0.01$

uS19-uS13 interface mutants exhibit a ligand binding profile indicative of unrotated ribosomes

Recent studies have suggested a correlation between ribosome rotational status and affinity of ribosomes for elongation factors. One study on uL16 mutants in yeast supported the model that unrotated ribosomes have higher affinity for ternary complex (eEF1A, aa-tRNA, and GTP) while rotated ribosomes have higher affinity for the translocase eEF2.⁵⁷ In another study, two uL2 mutants were shown to drive ribosomal rotational equilibrium toward the rotated state using the same criteria.⁵⁶ To test the consistency of this model, radiometric steady-state binding assays were utilized. (Figure 21) Ribosomes containing LGH112-114AAA exhibited a more than two-fold decrease in K_D for ternary complex (Figure 21B) and a two-fold decrease in K_D for acetylated aminoacyl tRNA compared to wild-type (Figure 21A). Ternary complex and ac-aa-tRNA binding for ribosomes containing QV104-105AA were both comparable to wild-type. (Figure 21A & 21B) Both mutants exhibited a nearly 2.5-fold increase in K_D for the translocase eEF2 which has a higher affinity for rotated ribosomes than unrotated ribosomes (Figure 21C). This increased affinity for A-site substrate (ternary complex) and decreased affinity for the translocase, eEF2, is indicative of a shift in the ribosomal rotational equilibrium toward the unrotated state.

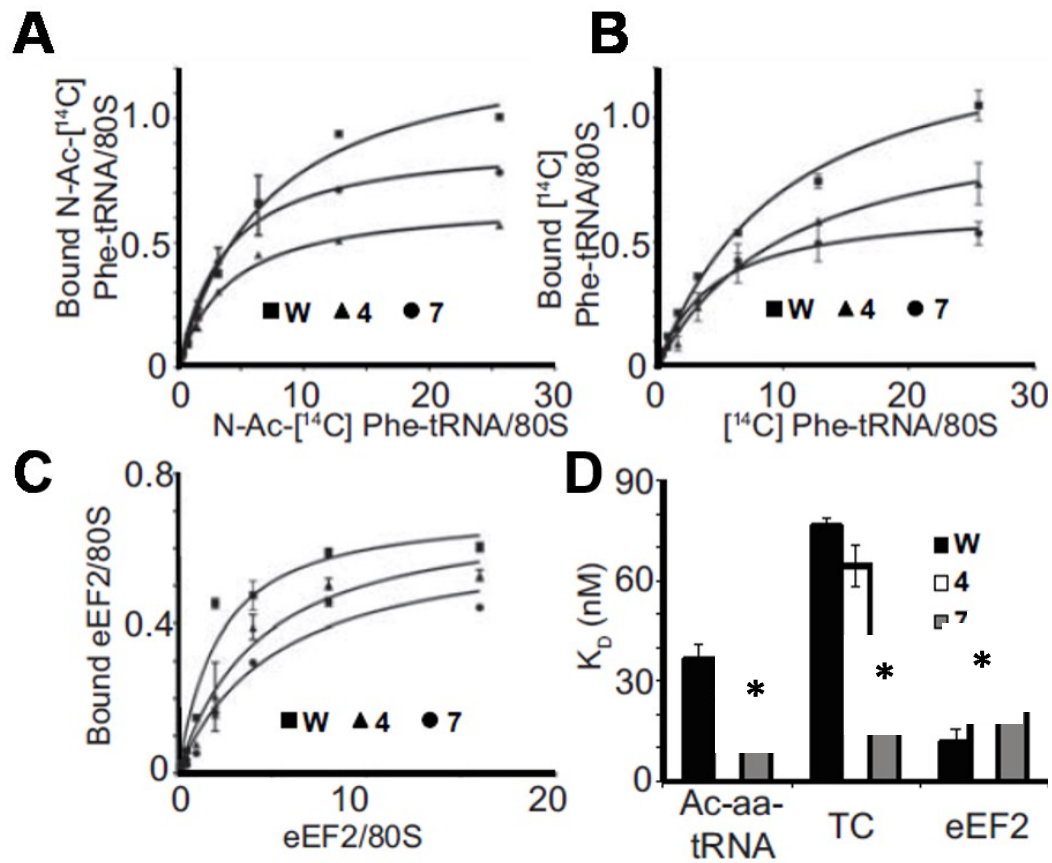


Figure 21: uS19/uS13 dimer interface mutants promote increased TC binding and decreased translocase binding.

(A) P-site tRNA binding: Salt-washed ribosomes were incubated for 10 minutes at 30°C with 2-fold dilutions of [¹⁴C]-ac-aa-tRNA and polyuridylic acid (Poly U). (B) A-site tRNA binding: Salt-washed ribosomes were incubated for 10 minutes at 30°C with 2-fold dilutions of pre-incubated ternary complex ([¹⁴C]-aa-tRNA•eEIF1A•GTP) and poly U. (C) eEF2 binding: Salt-washed ribosomes were incubated for 30 minutes at 30°C with 2-fold dilutions of purified eEF2, diphtheria toxin, and [¹⁴C]-NAD. In all three cases, binding was determined using liquid scintillation counting. (D) K_D values calculated using ligand depletion model in GraphPad Prism. **P* < 0.05, ***P* < 0.01

uS19/uS13 dimer interface mutants perturb the rotational equilibrium of ribosomes

High-throughput Selective 2'-Hydroxyl Acylation Analyzed by Primer Extension (hSHAPE) was utilized to determine the relative rotational status of uS19/uS13 dimer interface mutants. A previous study in yeast ribosomes utilized hSHAPE to establish a chemical reactivity profile of rotated and unrotated ribosomes based on two key bases in the B7a intersubunit bridge.⁵⁷ G913 of the 18S rRNA and A2207 of the 25S rRNA are known come in close contact in unrotated ribosomes and dissociate from one another in rotated ribosomes (Figure 22A). The involvement of these bases in such an interaction renders them inaccessible for chemical modification while their dissociation allows them to react with chemicals. The reactivity of G913 was probed using Kethoxal, a guanine specific chemical, while the reactivity of A2207 was probed using 1-methyl-7-nitroisatoic anhydride (1M7). Both QV104-105AA and LGH112-114AAA exhibited decreased reactivity of both B7a bridge residues (Figure 22B & C), indicative of a shift in the ribosomal rotational equilibrium toward the unrotated state.

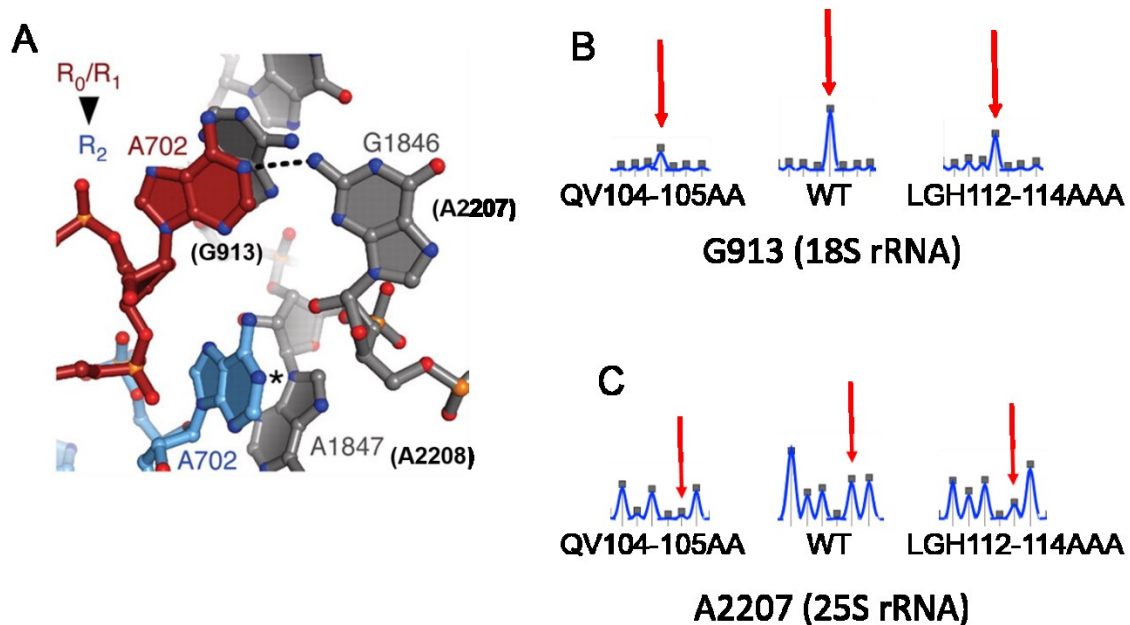


Figure 22: uS13/uS19 interface mutations perturb ribosomal rotational equilibrium

(A) In unrotated ribosomes, 18S base G913 and 25S base A2207 (A702 and G1846 in *E. coli*) interact while, in unrotated ribosomes, these bases “flip out” and are solvent accessible. Image credit: Zhang, et al.⁵⁴ (B) Kethoxal probing of G913 (18S rRNA) (C) 1M7 probing of A2207 (25S rRNA). Images created in ShapeFinder.⁶³

Discussion

While the ribosome is central to all life on earth, over the course of evolution significant differences between the three domains of life have emerged as their ribosomes have been subjected to different types of selective pressure. In prokaryotes and archaea, a single SSU protein, uS13, partners with H38 (the A-site finger) and uL5 to form the B1a and B1b/c bridges respectively. In eukaryotes, it appears that the SSU component was split into two separate proteins during the course of evolution. One of these, also known as uS13, only participates in bridge B1b/c with uL5 in eukaryotes. The other,

called uS19 (previously known as S15) is the SSU partner in the B1a bridge with H38. In this work, we explored potential advantages of this split by mutating residues at the uS19/uS13 interface and drawing phenotypic comparisons between mutant and wild-type ribosomes. We have shown that uS19/uS13 interface mutants are detrimental to ribosome structure and function.

We propose that eukaryotic ribosomes require a greater degree of flexibility due to their more complex biogenesis, eukaryote-specific structural rearrangements, and increased structural complexity. In prokaryotic ribosome biogenesis, all three precursor rRNA molecules are derived from one primary transcript while the four precursor rRNAs in eukaryotes are derived from two primary transcripts.⁶⁴ In addition, due to the lack of compartmentalization of prokaryotic cells, all cellular processes are colocalized. In fact, maturation of the primary transcript begins before transcription ends. Local secondary structures form co-transcriptionally and, as their binding sites emerge, ribosomal proteins bind the transcript. Eukaryotic ribosome biogenesis occurs in the nucleolus, nucleus, and cytoplasm. Eukaryotic ribosomes are larger and more complex with more proteins, rRNA helices, and eukaryote-specific expansion segments. Lastly, the SSU head region universally experiences the largest rearrangements of any part of the SSU throughout translation. However, in eukaryotic translation initiation, the initiation factors eIF1 and eIF1A induce an “open conformation” of the 40S subunit in which the head region interacts with the shoulder region clamping the incoming mRNA and locking the initiator tRNA onto the AUG codon.⁶⁵ This rearrangement does not occur in prokaryotic translation initiation because in prokaryotes, the AUG codon is positioned in the P-site by base pairing interactions between the Shine-Dalgarno sequence on the mRNA and the

anti-Shine Dalgarno sequence on the 16S rRNA.^{20,66,67} During the elongation cycle, as ribosomes rotate, the head region rotates 14° with respect to the rest of the SSU. While head swiveling is a universal rearrangement, recently another eukaryote-specific motion known as “subunit rolling” was identified in mammalian ribosomes.¹¹ Between the pre- and post-translocation stages, the SSU “rolls” or rotates along its long axis, orthogonal to the plane of intersubunit rotation. We hypothesize that with such an abundance of eukaryote-specific motions and structural elements, eukaryotic ribosomes require a greater degree of structural flexibility. As such, we suggest that the split of prokaryotic uS13 into eukaryotic uS13 and uS19 was selected for by the evolutionary process based on the increase in structural flexibility which it provides.

From atomic resolution structures of yeast ribosomes, we know that uS19 residues L₁₁₂GH₁₁₄ are nestled between uS13 and uS19 and appear to interact closely with both proteins (Figure 23A). Mutating these residues resulted in a decrease in ribosomal rotation and perturbation of the ribosomal rotational equilibrium favoring the unrotated state. We present a model in which L₁₁₂GH₁₁₄ act as the ball in a “ball-and-socket joint” allowing for a full range of motion between the two proteins (Figure 23B). With the head region of the SSU undergoing the largest structural rearrangements of any region throughout translation, we believe that this disruption of tightly interacting head region residues causes this “ball-and-socket joint” to stiffen, thus decreasing its range of motion and consequently, perturbing rotational equilibrium.

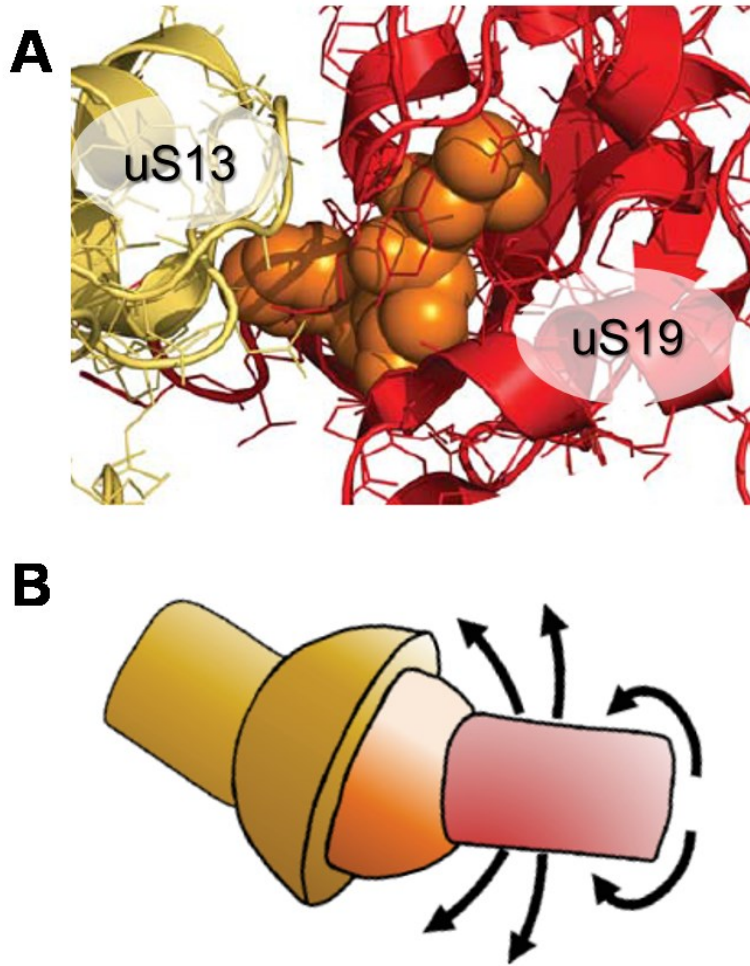


Figure 23: Residues $L_{112}GH_{114}$ act as the “ball” in a “ball-and-socket joint” providing added flexibility to the head region of the SSU

(A) $L_{112}GH_{114}$ (orange) is nestled in the core of uS19 (red) and interacts intimately with uS13 (yellow). Image created in PyMol from Yusupov (2011)¹² (B) ball-and-socket joint model of uS13 (yellow) and uS19 (red) with $L_{112}GH_{114}$ (orange) in the center as the “ball” allowing for a full range of motion between the two proteins.

Without this added flexibility, which is necessary for proper ribosome function, yeast cellular fitness is reduced, translational fidelity is decreased, and ribosomal rotational equilibrium becomes disrupted. LGH112-114AAA is the only mutant in this

study with a slow growth phenotype at 30°C and no growth at 37°C. In addition, LGH112-114AAA is sensitive to paromomycin, a small molecule translation inhibitor. Paromomycin binds to the SSU decoding center, occupying critical decoding center bases which are involved in stabilizing cognate ternary complex in the A-site. Mutants with paromomycin sensitivity are expected to have difficulty differentiating between cognate and near-cognate codons. Indeed, LGH112-114AAA exhibited a 5-fold increase of suppression of missense codons over wild-type, consistent with the paromomycin sensitivity phenotype. Three lines of evidence support the shift in rotational equilibrium toward the unrotated state and these data are consistent with two previous ribosomal protein mutant studies. First of all, as the ribosome transits through elongation, it experiences two extreme states of rotation termed “rotated” and “unrotated”. Unrotated ribosomes are substrates for ternary complex while rotated ribosomes are substrates for the translocase eEF2. LGH112-114AAA exhibited increased affinity for ternary complex and decreased affinity for the translocase eukaryotic elongation factor 2 (eEF2) consistent with previous studies.^{56,57} These results open the door for additional queries about how ribosomal proteins affect the other stages of translation.

In eukaryotes, a key feature of translational fidelity at initiation is the ability of the head of the SSU to swivel and lock the initiator tRNA onto the initiator codon. Due to the previously described translational fidelity defects exhibited by LGH112-114AAA, we posit that this mutant would also exhibit initiation defects, specifically a Sui⁻ (suppressor of initiation codon mutant) phenotype.^{19,68} Overall, studying ribosomal proteins in this manner is crucial as ribosomes are the target of many antibiotics. Additionally, the effects of uS19/uS13 interface mutations described in this study could

have broader implications in understanding the progression of diseases caused by mutated ribosomes (ribosomopathies).

Chapter 3: Materials and Methods

Strains, plasmids, and media

The gene encoding S15, *RPS15*, and its native 5' and 3' untranslated regions (UTRs) were amplified from *S. cerevisiae* genomic DNA. This PCR product was cloned into pRS313, a *HIS3*-based low-copy expression vector.

Mutations in the *RPS15* ORF of pRPS15-HIS3 were generated by oligonucleotide site-directed mutagenesis using the Quikchange XL site-directed mutagenesis kit (Stratagene, Madison, WI, USA). Plasmids were amplified in the DH5 α strain of *E. coli*. Mutations were introduced into *RPS15* knockout yeast strain JD1346 (*his3 Δ 1*; *leu2 Δ 0*; *ura3 Δ 0*; *YOL040c::KanMX4*; *pFL38(Pgal)::RPS15*; *URA3*) using a standard lithium acetate yeast transformation protocol⁶⁹ and subsequent 5-FOA plasmid shuffle.⁷⁰

Genetic Assays

Standard 10-fold dilution spot assays were used as a qualitative measure of sensitivity to temperature and small molecule translational inhibitors. Dilution spot assays were performed as previously described.⁶¹ Briefly, yeast were grown in synthetic histidine deletion media (-His) to logarithmic growth phase. Serial dilutions were made from 10⁵ to 1 colony-forming unit (CFU) per 2.2 μ l and spotted on -His agar media. For pharmacogenetic assays, 10 μ g/ml of anisomycin and 45 μ g/ml of paromomycin were added to -His agar media and the plates were incubated at 20°C for 3-5 days. For

temperature sensitivity the plates were incubated in cold (20°C), optimal growth temperature for yeast (30°C) and elevated temperature (37°C).

The killer maintenance assay is a qualitative assay of translational fidelity and was also performed as previously described.⁴⁰ Briefly, cells were replica plated on 4.7 MB plates covered in a lawn of killer sensitive (K⁻) cells and plates were incubated at 20°C for 2-3 days. Killer phenotype was detected as a zone of growth inhibition around the patch of test cells. Mutants were scored based on their ability to maintain killer relative to wild-type.

Quantitative Translational Fidelity Assays

Bicistronic luminescent reporter assays were employed to quantitatively probe programmed +1 ribosomal frameshifting (+1 PRF), -1 PRF, suppression of the nonsense UAA codon, and missense suppression. In the missense reporter, the AGC serine codon at position 218 in the firefly luciferase catalytic site is replaced with an AGA arginine codon. The dual luciferase assays were performed and data was analyzed as previously described. In summary, strains are first transformed with reporters for each of the aforementioned assays. For example, the -1 PRF bicistronic reporter contains firefly and renilla luciferase ORFs with the renilla ORF in the -1 frame with respect to that of firefly. Between the ORFs is the -1 frameshift signal sequence from HIV-1. After transformation with reporter plasmids, the strains were grown in synthetic uracil deletion media (-Ura) to mid-log phase and lysed (lysis buffer: 1X PBS, 1 mM phenylmethylsulfonyl fluoride (PMSF)). Firefly and renilla luciferase substrate solutions were prepared from a Dual Luciferase Reporter Assay Kit (Promega, Madison, WI). The lysates were read in a

Promega GloMax®-Multi Detection System Luminometer. Data analysis was performed as previously described.⁷¹

Ribosome Purification

Ribosomes were isolated from mutant yeast strains for in vitro ligand binding assays. Cultures were grown in 5 ml of YPAD media and inoculated in 500 ml of YPAD overnight in a 30°C shaker and grown to mid-log phase. Cells were incubated at 4°C for 1 hour to allow ribosomes to dissociate from mRNA transcripts, but remain intact. Cells were harvested by centrifugation in a ThermoScientific™ Sorvall™ Legend RT Plus Centrifuge and washed twice with ribosome purification binding buffer (20 mM HEPES-KOH pH 7.6, 60 mM NH₄Cl, 5 mM Mg(CH₃COO)₂, 2 mM DTT). Cells were resuspended in 1 ml of binding buffer per gram of cells and lysed in 2 ml screw cap vials half-filled with beads using a minibead beater. Lysates were clarified by centrifugation in a Beckman Coulter Optima™ XE-90 Ultracentrifuge at 30,000g using an SW-41Ti rotor at 4°C for 30 minutes. The supernatant was separated from the pelleted cell debris and ribosomes were isolated by affinity purification using Sulfolink beads (Pierce, Rockford, IL). The sulfolink beads were first incubated on ice after addition of supernatant for 30 minutes. The column was centrifuged at 1000 rpm momentarily followed by two washes with binding buffer. Ribosomes were eluted from the resin in 8 ml of elution buffer (20 mM HEPES-KOH pH 7.6, 60 mM NH₄Cl, 500 mM KCl, 10 mM Mg(CH₃COO)₂, 2 mM DTT, 0.5 mg/ml heparin). Eluted ribosomes were treated with 1mM each puromycin and GTP for 30 minutes at 30°C to ensure removal of endogenous peptidyl tRNA, mRNA, and soluble factors. Ribosome solution was layered atop 22 ml

of glycerol cushion buffer (50 mM HEPES-KOH pH 7.6, 10 mM Mg(CH₃COO)₂, 60 mM NH₄Cl, 500 mM KCl, 2 mM DTT, 25% glycerol) and pelleted by centrifugation overnight at 100,000g at 4°C in a SW-32Ti rotor. Pellets were washed in 1 ml of storage buffer (50 mM HEPES-KOH pH 7.6, 5 mM Mg(CH₃COO)₂, 50 mM NH₄Cl, 1 mM DTT, 25% glycerol) and resuspended in 200-400 µl of storage buffer. Ribosome concentrations were determined using a spectrophotometer (1 ODU at 260 nm = 20 pmoles of ribosomes). The ribosomes were stored at -80°C in 500 picomole aliquots until needed for ligand binding assays.

Ligand Binding Assays

6X-His-tagged eukaryotic elongation factor 2 (eEF2) was purified from *Saccharomyces cerevisiae* strain TKY675, a generous gift from Dr. Terry Kinzy. Cells were grown overnight in 5 ml of YPAD and cultures were inoculated in 500 ml the following night. Once cell growth reached logarithmic phase (OD₅₉₅ = 0.6-1), cells were harvested and washed with ultrapure water. Cells were resuspended in 1 ml of binding buffer (20 mM Sodium Phosphate Buffer pH 7.4, 500 mM NaCl, 20 mM Imidazole) per 1 gram of cells and lysed in a minibead beater using glass beads. The resulting lysate was centrifuged in an ultracentrifuge fixed with an SW-32Ti rotor at 32,000 RPM for 3 hours at 4°C. The supernatant was promptly removed from the cell debris and run on Ni-NTA agarose affinity columns. Following purification, residual imidazole was removed by buffer exchange (100 mM Tris-HCl pH 7.5, 5 mM EDTA). The protein was stored in 50 µl aliquots in a -80°C freezer.

Aminoacylated and acetylated aminoacylated tRNAs ($[^{14}\text{C}]\text{Phe-tRNA}^{\text{Phe}}$ and N-Ac- $[^{14}\text{C}]\text{Phe-tRNA}^{\text{Phe}}$, respectively) were synthesized from CCA-repaired phenylalanyl tRNAs and purified by high performance liquid chromatography (HPLC) as previously described.⁷² For A-site ligand binding assay, 100 picomoles of purified ribosomes were incubated for 30 minutes at 30°C with polyuridylic acid (Poly U), cold phenylalanyl tRNA, and 4X Binding Buffer (80 mM Tris-HCl pH 7.4, 160 mM NH_4Cl , 15 mM $\text{Mg}(\text{CH}_3\text{COO})_2$, 2 mM spermidine, 0.5 mM spermine, 6 mM β -mercaptoethanol) to a total volume of 300 μl . Ternary complex was formed by combining 512 picomoles of $[^{14}\text{C}]\text{Phe-tRNA}^{\text{Phe}}$, GTP, Soluble protein factors, and 4X Binding Buffer to a final volume of 270 μl and incubating for 30 minutes at 30°C. Eight two-fold serial dilutions of ternary complex mix were prepared such that the concentration of ternary complex in each tube was 128 picomoles, 64 picomoles, 32 picomoles, etc. 15 μl of the ribosome mix was added to each tube and the ternary complex + ribosome mix was incubated for 30 minutes at 30°C. The solutions were then poured onto moistened Millipore HA 0.45 micron nitrocellulose filters and incorporated radioactivity was determined by scintillation counting.

For P-site ligand binding, 100 picomoles of purified ribosomes were incubated for 10 minutes at 30°C with polyuridylic acid (Poly U), and 4X Binding Buffer (80 mM Tris-HCl pH 7.4, 160 mM NH_4Cl , 11 mM $\text{Mg}(\text{CH}_3\text{COO})_2$, 2 mM spermidine, 0.5 mM spermine, 6 mM β -mercaptoethanol) to a total volume of 300 μl . tRNA mix was formed by combining 512 picomoles of N-Ac- $[^{14}\text{C}]\text{Phe-tRNA}^{\text{Phe}}$, and 4X Binding Buffer to a final volume of 270 μl and incubating for 10 minutes at 30°C. Eight two-fold serial dilutions of tRNA mix were prepared such that the concentration of tRNA in each tube

was 128 picomoles, 64 picomoles, 32 picomoles, etc. 15 μ l of the ribosome mix was added to each tube and the tRNA + ribosome mix was incubated for 30 minutes at 30°C. The solutions were then poured onto moistened Millipore HA 0.45 micron nitrocellulose filters and incorporated radioactivity was determined by scintillation counting. Elongation factor 2 (eEF2) binding was performed as previously described.⁷³ Binding data were analyzed and K_D values were calculated via single binding site with ligand depletion models using GraphPad Prism software.

Ribosomal RNA Chemical Modification and Analysis

For chemical modification of rRNA, 50 picomoles of ribosomes were first reactivated with 50 μ l of 2X SHAPE buffer (160 mM HEPES-KOH pH 7.5, 100 mM NaCl, 5 mM Mg(CH₃COO)₂, 6 mM β -mercaptoethanol) at 30°C for 10 minutes. For the SHAPE reaction, 75 μ l of 1X SHAPE buffer and 12.5 μ l of either DMSO (negative control) or 1-methyl-7-nitroisatoic anhydride (1M7) was added to 50 μ l of reactivated ribosomes. The mixture was incubated for 10 minutes at 30°C and ethanol precipitated overnight. The modified rRNA was then purified using an RNAqueous micro kit (LifeTechnologies, Grand Island, NY) and used in primer extension reactions. Primer extension was performed as previously described and 10 μ l samples in Hi-Di Formamide were sent to Genewiz (Frederick, MD) for capillary sequencing. Data was analyzed using ShapeFinder.⁶³

Molecular RNA (mRNA) Abundance Assay

Quantitative Real-Time PCR (qRT-PCR) was utilized to measure mRNA abundance. Procedure was performed as previously described.⁷⁴ Briefly, total RNA was isolated from liquid yeast culture grown to mid-logarithmic phase using Trizol reagent. Following ethanol precipitation, complementary DNA (cDNA) was synthesized from isolated RNA. EST3 (test) and U3 (reference) oligonucleotides were used in qRT-PCR experiments. The students t-test for two-tailed P value calculations was used for statistical analysis.

Chapter 4: Conclusions and Future Directions

Ribosomes are complex nanomachines comprised of rRNA and protein molecules which must seamlessly cooperate. While most ribosomal elements are universally conserved, the evolutionary process has selected for several features which enhance eukaryotic ribosome function. This study has highlighted one such structural feature which provides a greater degree of structural flexibility in one of the most dynamic regions of the ribosome. We posit that eukaryotic ribosomes require a greater degree of structural flexibility than their prokaryotic homologs due to their increased size and complexity, differences in their respective processes of biogenesis, and increased complexity of their translation initiation and elongation. From a broader standpoint, we have also shown that proper ribosome function is very sensitive to minor alterations to the ribosomal machinery. Mutating three residues in one of the nearly 80 ribosomal proteins resulted in dramatic alterations of cell growth, translational fidelity, and overall ribosome function.

Here, we demonstrated that by introducing mutations in critical residues of the flexible SSU head region, ribosomes experience a shift in rotational equilibrium. The head region of the SSU experiences the largest rearrangements of any part of the SSU. Additionally, the uS19/uS13 interface has been previously described as a critical interaction in the head region. As ribosomes transit through the elongation cycle, several trans-acting factors are required, each utilizing the same binding pockets. It is indeed intriguing that the ribosome is a ribozyme which binds a variety of structural mimics in the same binding sites. Previous studies have indicated that the ribosome has a so-called “temporal affinity” for its various ligands.⁵⁷ That is, depending on its current status, a

ribosome could have varying affinities for each of its ligands. Interestingly, this affinity is an intrinsic property of the ribosomal environment which is created by the individual ribosomal components. Ribosomes are merely composites of rRNA molecules and proteins. These individual elements are what gives the ribosome its capacity for binding its particular subset of trans-acting factors. As ribosomes rotate, it is the dynamic, individual elements of the ribosome which associate and dissociate from one another and drive this rotation. As the SSU head swivels at the neck region and the SSU rolls along its long axis, there is interplay between the individual rRNA molecules and proteins which drives and stabilizes these motions. As these highly dynamic elements rotate and bend throughout translation, interacting with nearby elements, their attractive and repulsive forces cascade throughout the ribosome, resulting in effects on distal regions. A previous study of eukaryotic ribosomal protein uL5 showed that uL5 mutations had long-ranging effects on ribosome structure over as many as 100 Å away from the protein.^{4,61} Therefore, the critical ability of ribosomes to rotate as they transit through the translational process is provided by each of these individual elements. By introducing mutations in the uS13/uS19 interface of uS19, we have demonstrated that disturbing the intrinsic communication pathways of the ribosome perturbs ribosomal rotation and overall function.

Medical Impact: A relatively new class of diseases known as ribosomopathies are of particular interest to translational control researchers. Ribosomopathies are diseases which arise as a result of ribosomal mutations. One such ribosomopathy, Diamond Blackfan Anemia (DBA) results from ribosomal mutations in more than 50% of affected patients. Protein synthesis is a crucial physiological process. While not all

ribosomal proteins are essential for cellular viability, ribosomal proteins do play key roles in ribosome biogenesis and, as this study has illustrated, mutated ribosomal proteins lead to defective ribosomes which are not capable of maintaining translational fidelity. It is important that we broaden our understanding of ribosomal proteins to be able to combat this recently characterized class of diseases.

Future Directions: Presented here is a reverse genetics approach to determining the function of the uS13/uS19 interface by mutating uS19 residues which interact with uS13. To further support these findings, the dimer interface of uS13 should be assayed in the same manner. In this study, we postulate that the movement of uS13 and uS19 about residues L₁₁₂GH₁₁₄ resembles a ball-and-socket joint. Förster Resonance Energy Transfer (FRET) is a biophysical method in which donor/acceptor fluorophore pairs can be bound to the distal end of each protein. Ribosome complexes containing ligands representing each stage of translation can be formed and FRET can be used to determine how these two proteins move with respect to one another throughout the elongation cycle. Additionally, in order to increase our understanding of how ribosomal protein mutations affect structure, cryo-electron microscopy (cryo-EM) can be employed to visualize structural changes of mutant ribosomes. Finally, in this study, we posit that the uS13/uS19 interface region is critical because it was selected for by the evolutionary process. By this logic, other eukaryote-specific elements of ribosomes must also harbor residues important for eukaryotic ribosomal function or structural stability. These elements, such as expansion segments, should also be assayed in a similar manner.

Appendix 1: List of Synthetic Oligonucleotide Primers

Name	Sequence
S15_S18_polyA_1	5'-GTCGTCGGTATCTACgctgctgctgctgctCAAGTTG AAATCAGACC-3'
S15_S18_polyA_2	5'-GGCTTTC AACGCTGCTGCTGCTGCTGCTGAAATG TTGGGTC ACTATTTGG-3'
S15_S18_polyA_3	5'-CCAAGTTGAAATCAGACCgctgctgctgctTATTT GGGTGAATTC-3'
S15_ASF_polyA_1	5'-CTGCCCCAgctgctgctgctgctCCAGTCAGAACCCAC ATGAGAAAC-3'
S15_ASF_polyA_2	5'-GCCCCAGAAAAGCCAGCTCCAGTCAGAACCCA CATGAGAAACATGATC-3'
S15_S18_ASF_REV	5'-GCGGCCGCTCTAGAACTAGTGGATCCGGTCC ACAGGATGAACTAAATAGC-3'
S15_S18_region_1	5'-CGGTTCCGTCGTCGGTATCTACgctgctAAGGC TTTCAACCAAGTTGAAATCAGACC-3'
S15_S18_region_2	5'-CCGTCGTCGGTATCTACAACGGTgctgctTTC AACCAAGTTGAAATCAGACCAG-3'
S15_S18_region_3	5'-CCGTCGTCGGTATCTACAACGGTAAGGCT gctgctCAAGTTGAAATCAGACCAG-3'
S15_S18_region_4	5'-CGTCGGTATCTACAACGGTAAGGCTTTC ACgctgctGAAATCAGACCAGAAATGTTGGG-3'

S15_S18_region_5	5'-CGTCGGTATCTACAACGGTAAGGCTTTCAAC CAAGTTgctgctAGACCAGAAATGTTGGG-3'
S15_S18_region_6	5'-CGTCGGTAAGGCTTTCAACCAAGTTGAAA TCgctgctGAAATGTTGGGTCACTATTTGGG-3'
S15_S18_region_7	5'-CGGTAAGGCTTTCAACCAAGTTGAAATCAGA CCAgctgctTTGGGTCACTATTTGGG-3'
S15_S18_region_8	5'-CCAAGTTGAAATCAGACCAGAAATGgctgctgct TATTTGGGTGAATTCTCC-3'

Appendix 2: Yeast Strain List

Strain	Genotype
5X47	<i>MATa/MATa his1/+ trp1/+ ura3/+ K</i>
JD1346	<i>(GAL-RPS15) his3Δ1; leu2Δ0; ura3Δ0; YOL040c::KanMX4; pFL38(P_{gal}::RPS15; URA3)</i>
JD1529	<i>MAT α((GAL-RPS15) his3Δ1; leu2Δ0; ura3Δ0; YOL040c::KanMX4; pFL38(P_{gal}::RPS15; URA3)) [L-A HN M1] [psi-]</i>
JD1530	<i>MATa (GAL-RPS18) his3Δ1; leu2Δ0; ura3Δ0; YDR450w::KanMX4; YML026c::KanMX4; pFL38(P_{gal}::RPS18A; URA3) [L-A HN M1] [psi-]</i>
JD1693	<i>MAT α((GAL-RPS15) his3Δ1; leu2Δ0; ura3Δ0; YOL040c::KanMX4; pFL38(P_{gal}::RPS15; URA3)) [L-A HN M1] [psi-]pRPS15 (NG98-99AA)-HIS3</i>
JD1694	<i>MAT α((GAL-RPS15) his3Δ1; leu2Δ0; ura3Δ0; YOL040c::KanMX4; pFL38(P_{gal}::RPS15; URA3)) [L-A HN M1] [psi-]pRPS15 (KA100-101AA)-HIS3</i>
JD1695	<i>MAT α((GAL-RPS15) his3Δ1; leu2Δ0; ura3Δ0; YOL040c::KanMX4; pFL38(P_{gal}::RPS15; URA3)) [L-A HN M1] [psi-]pRPS15 (FN102-103AA)-HIS3</i>
JD1696	<i>MAT α((GAL-RPS15) his3Δ1; leu2Δ0; ura3Δ0; YOL040c::KanMX4; pFL38(P_{gal}::RPS15; URA3)) [L-A HN</i>

	<i>M1] [psi-]pRPS15 (QV104-105AA)-HIS3</i>
JD1697	<i>MAT α((GAL-RPS15) his3Δ1; leu2Δ0; ura3Δ0; YOL040c::KanMX4; pFL38(Pgal::RPS15; URA3)) [L-A HN M1] [psi-]pRPS15 (E1106-107AA)-HIS3</i>
JD1698	<i>MAT α((GAL-RPS15) his3Δ1; leu2Δ0; ura3Δ0; YOL040c::KanMX4; pFL38(Pgal::RPS15; URA3)) [L-A HN M1] [psi-]pRPS15 (RP108-109AA)-HIS3</i>
JD1699	<i>MAT α((GAL-RPS15) his3Δ1; leu2Δ0; ura3Δ0; YOL040c::KanMX4; pFL38(Pgal::RPS15; URA3)) [L-A HN M1] [psi-]pRPS15 (LGH112-114AA)-HIS3</i>
JD1701	<i>MAT α((GAL-RPS15) his3Δ1; leu2Δ0; ura3Δ0; YOL040c::KanMX4; pFL38(Pgal::RPS15; URA3)) [L-A HN M1] [psi-]pRPS15 (ENEKP69-73AAAAA)-HIS3</i>
JD1702	<i>MAT α((GAL-RPS15) his3Δ1; leu2Δ0; ura3Δ0; YOL040c::KanMX4; pFL38(Pgal::RPS15; URA3)) [L-A HN M1] [psi-]pRPS15 (APVR74-77AAAA)-HIS3</i>

Appendix 3: Genetic and Functional Analyses of B1a Bridge Mutants in uS19

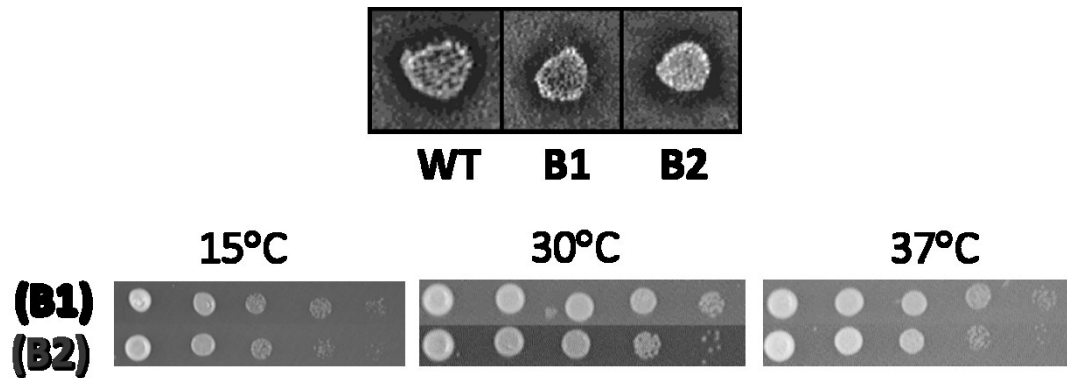


Figure A3.1: Summary of Genetic Assays of Bridge Mutants

(TOP) Killer assays of wild-type (WT), ENEKP69-73AAAAA (B1), and APVR74-77AAAAA (B2). Assay was performed as described in Chapter 3. Briefly, cells were replica plated on 4.7 MB plates covered in a lawn of killer sensitive (K^-) cells and plates were incubated at 20°C for 2-3 days. Killer phenotype was detected as a zone of growth inhibition around the patch of test cells. Mutants were scored based on their ability to maintain killer relative to wild-type. (BOTTOM) Temperature sensitivity was assayed using standard 10-fold serial dilution spots and incubating plates at the indicated temperatures. Assay was performed as described in Chapter 3. Briefly, yeast were grown in synthetic histidine deletion media (-His) to logarithmic growth phase. Serial dilutions were made from 10^5 to 1 colony-forming unit (CFU) per 2.2 μ l and spotted on -His agar media. The plates were incubated in cold (20°C), optimal growth temperature for yeast (30°C) and elevated temperature (37°C).

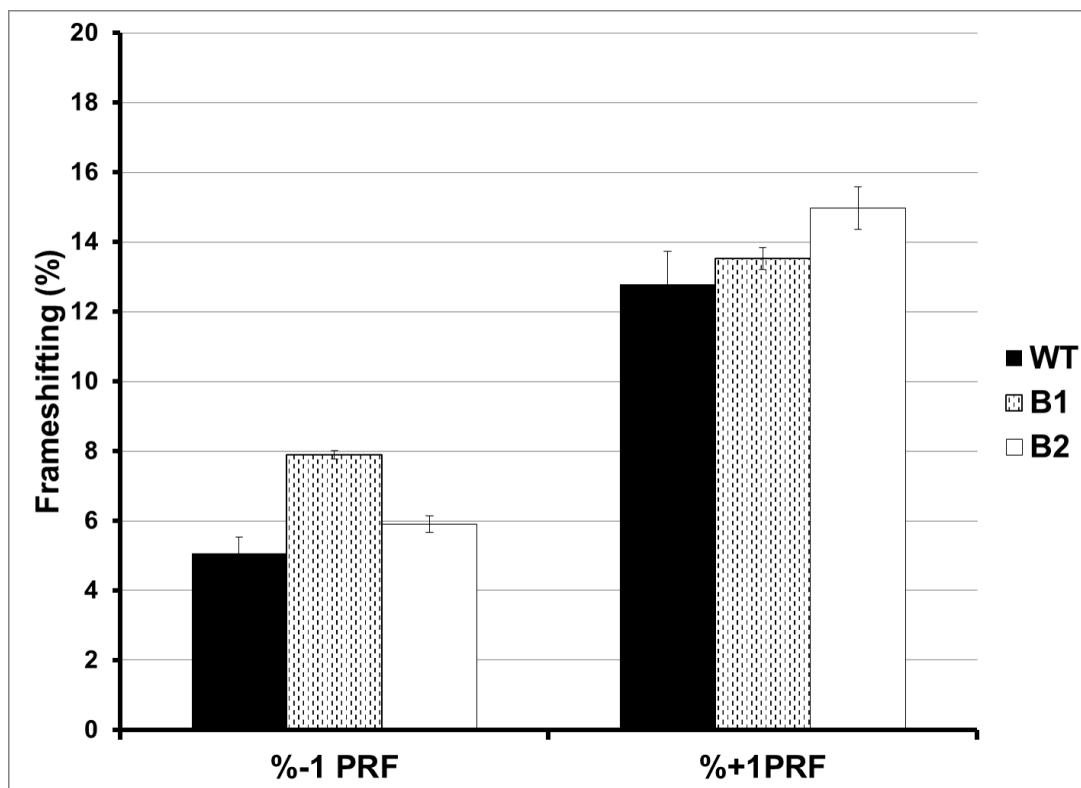


Figure A3.2: Programmed -1 and +1 Ribosomal Frameshifting Assays of Bridge Mutants

Wild-type (WT), ENEKP69-73AAAAA (B1), and APVR74-77AAAA (B2). Assays were performed as described in Chapter 3. Briefly, strains are first transformed with reporters for each of the aforementioned assays. For example, the -1 PRF bicistronic reporter contains firefly and renilla luciferase ORFs with the renilla ORF in the -1 reading frame with respect to that of firefly. Between the ORFs is the -1 frameshift signal sequence from HIV-1. The +1 PRF reporter plasmid contains the Ty1 +1 PRF signal with the downstream renilla ORF in the +1 reading frame with respect to that of firefly. After transformation with reporter plasmids, the strains were grown in synthetic uracil deletion media (-Ura) to mid-log phase and lysed (lysis buffer: 1X PBS, 1 mM phenylmethylsulfonyl fluoride (PMSF)). Firefly and renilla luciferase substrate solutions were prepared from a Dual Luciferase Reporter Assay Kit (Promega, Madison, WI). The lysates were read in a Promega GloMax®-Multi Detection System Luminometer.

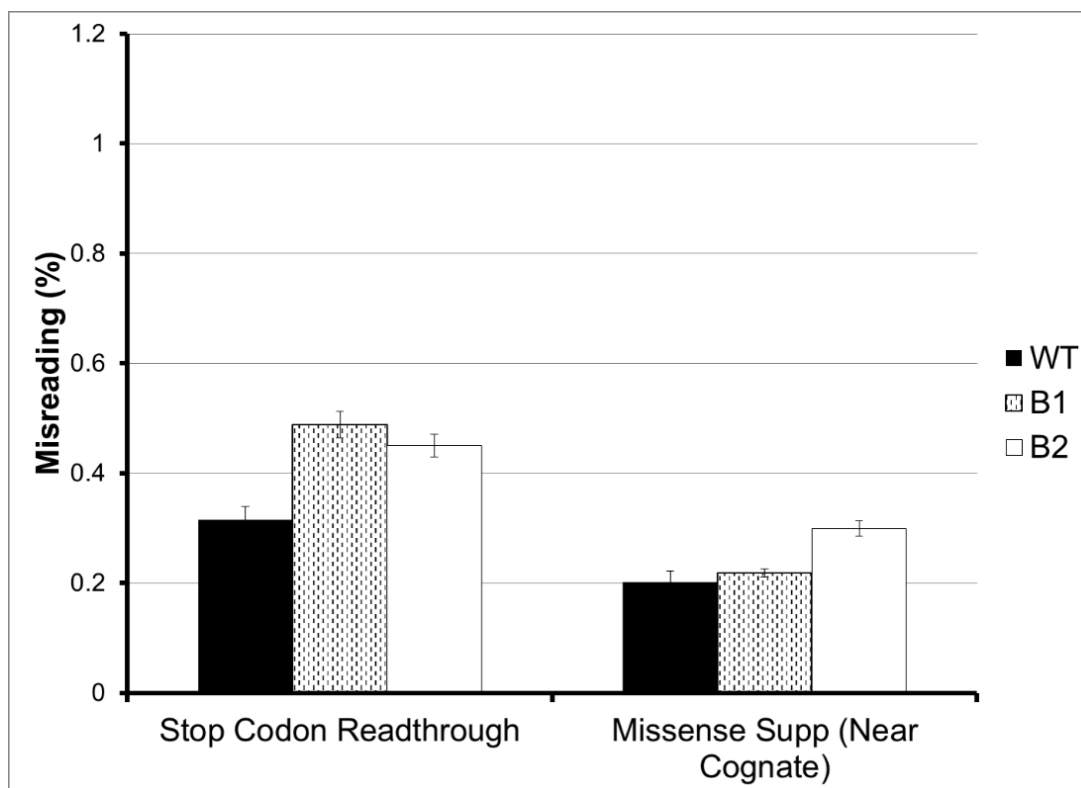


Figure A3.3: Missense and Nonsense Codon Suppression Assay Results for Bridge Mutants

Wild-type (WT), ENEKP69-73AAAAA (B1), and APVR74-77AAAA (B2). Assays were performed as described in Chapter 3. Briefly, strains are first transformed with reporters for each of the aforementioned assays. In the missense reporter, the AGC serine codon at position 218 in the firefly luciferase catalytic site is replaced with a near-cognate AGA arginine codon. In the stop codon readthrough bicistronic reporter, renilla and firefly luciferase ORFs are separated by a stop codon. After transformation with reporter plasmids, the strains were grown in synthetic uracil deletion media (-Ura) to mid-log phase and lysed (lysis buffer: 1X PBS, 1 mM phenylmethylsulfonyl fluoride (PMSF)). Firefly and renilla luciferase substrate solutions were prepared from a Dual Luciferase Reporter Assay Kit (Promega, Madison, WI). The lysates were read in a Promega GloMax®-Multi Detection System Luminometer.

Bibliography

1. Wimberly, B. T. *et al.* Structure of the 30S ribosomal subunit. *Nature* **407**, 327–39 (2000).
2. Schluenzen, F. *et al.* Structure of Functionally Activated Small Ribosomal Subunit at 3.3 Å Resolution. *Cell* **102**, 615–623 (2000).
3. Ban, N., Nissen, P., Hansen, J., Moore, P. B. & Steitz, T. A. The complete atomic structure of the large ribosomal subunit at 2.4 Å resolution. *Science* **289**, 905–20 (2000).
4. Rhodin, M. H. J. & Dinman, J. D. An extensive network of information flow through the B1b/c intersubunit bridge of the yeast ribosome. *PLoS One* **6**, e20048 (2011).
5. Planta, R. J. & Mager, W. H. The list of cytoplasmic ribosomal proteins of *Saccharomyces cerevisiae*. *Yeast* **14**, 471–7 (1998).
6. Lodish, H. *et al.* Molecular Cell Biology. (2000). at <http://www.ncbi.nlm.nih.gov/books/NBK21475/>
7. Jenner, L. *et al.* Crystal structure of the 80S yeast ribosome. *Curr. Opin. Struct. Biol.* **22**, 759–67 (2012).
8. Ogle, J. M. *et al.* Recognition of cognate transfer RNA by the 30S ribosomal subunit. *Science* **292**, 897–902 (2001).
9. Julián, P. *et al.* Structure of ratcheted ribosomes with tRNAs in hybrid states. *Proc. Natl. Acad. Sci. U. S. A.* **105**, 16924–7 (2008).
10. Frank, J. & Agrawal, R. K. A ratchet-like inter-subunit reorganization of the ribosome during translocation. *Nature* **406**, 318–22 (2000).
11. Budkevich, T. V *et al.* Regulation of the mammalian elongation cycle by subunit rolling: a eukaryotic-specific ribosome rearrangement. *Cell* **158**, 121–31 (2014).
12. Ben-Shem, A. *et al.* The structure of the eukaryotic ribosome at 3.0 Å resolution. *Science* **334**, 1524–9 (2011).
13. Noller, H. F. RNA structure: reading the ribosome. *Science* **309**, 1508–14 (2005).
14. Granneman, S. & Baserga, S. J. Ribosome biogenesis: of knobs and RNA processing. *Exp. Cell Res.* **296**, 43–50 (2004).

15. Fromont-Racine, M., Senger, B., Saveanu, C. & Fasiolo, F. Ribosome assembly in eukaryotes. *Gene* **313**, 17–42 (2003).
16. Hinnebusch, A. G. Molecular mechanism of scanning and start codon selection in eukaryotes. *Microbiol. Mol. Biol. Rev.* **75**, 434–67, first page of table of contents (2011).
17. Kozak, M. Pushing the limits of the scanning mechanism for initiation of translation. *Gene* **299**, 1–34 (2002).
18. Hinnebusch, A. G. The scanning mechanism of eukaryotic translation initiation. *Annu. Rev. Biochem.* **83**, 779–812 (2014).
19. Hinnebusch, A. G., Dever, T. E. & Asano, K. Mechanism of Translation Initiation in the Yeast *Saccharomyces cerevisiae*. *Cold Spring Harbor Monograph Archive* **48**, 225–268 (2007).
20. Kozak, M. Initiation of translation in prokaryotes and eukaryotes. *Gene* **234**, 187–208 (1999).
21. Kozak, M. How do eucaryotic ribosomes select initiation regions in messenger RNA? *Cell* **15**, 1109–1123 (1978).
22. Dever, T. E. & Green, R. The elongation, termination, and recycling phases of translation in eukaryotes. *Cold Spring Harb. Perspect. Biol.* **4**, a013706 (2012).
23. Demeshkina, N., Jenner, L., Westhof, E., Yusupov, M. & Yusupova, G. A new understanding of the decoding principle on the ribosome. *Nature* **484**, 256–9 (2012).
24. Rodnina, M. V, Fricke, R., Kuhn, L. & Wintermeyer, W. Codon-dependent conformational change of elongation factor Tu preceding GTP hydrolysis on the ribosome. *EMBO J.* **14**, 2613–9 (1995).
25. Rodnina, M. V & Wintermeyer, W. Ribosome fidelity: tRNA discrimination, proofreading and induced fit. *Trends Biochem. Sci.* **26**, 124–130 (2001).
26. Rodnina, M. V & Wintermeyer, W. Fidelity of aminoacyl-tRNA selection on the ribosome: kinetic and structural mechanisms. *Annu. Rev. Biochem.* **70**, 415–35 (2001).
27. Schmeing, T. M., Huang, K. S., Strobel, S. a & Steitz, T. a. An induced-fit mechanism to promote peptide bond formation and exclude hydrolysis of peptidyl-tRNA. *Nature* **438**, 520–524 (2005).

28. Alkalaeva, E. Z., Pisarev, A. V, Frolova, L. Y., Kisselev, L. L. & Pestova, T. V. In vitro reconstitution of eukaryotic translation reveals cooperativity between release factors eRF1 and eRF3. *Cell* **125**, 1125–36 (2006).
29. Jackson, R. J., Hellen, C. U. T. & Pestova, T. V. Termination and post-termination events in eukaryotic translation. *Adv. Protein Chem. Struct. Biol.* **86**, 45–93 (2012).
30. Gao, N. *et al.* Mechanism for the disassembly of the posttermination complex inferred from cryo-EM studies. *Mol. Cell* **18**, 663–74 (2005).
31. Dunkle, J. A. *et al.* Structures of the bacterial ribosome in classical and hybrid states of tRNA binding. *Science* **332**, 981–4 (2011).
32. Schwartz, D. E., Tizard, R. & Gilbert, W. Nucleotide sequence of rous sarcoma virus. *Cell* **32**, 853–869 (1983).
33. Jacks, T. *et al.* Characterization of ribosomal frameshifting in HIV-1 gag-pol expression. *Nature* **331**, 280–3 (1988).
34. Marra, M. A. *et al.* The Genome sequence of the SARS-associated coronavirus. *Science* **300**, 1399–404 (2003).
35. Wills, N. M., Moore, B., Hammer, A., Gesteland, R. F. & Atkins, J. F. A functional -1 ribosomal frameshift signal in the human paraneoplastic Ma3 gene. *J. Biol. Chem.* **281**, 7082–8 (2006).
36. Manktelow, E., Shigemoto, K. & Brierley, I. Characterization of the frameshift signal of Edr, a mammalian example of programmed -1 ribosomal frameshifting. *Nucleic Acids Res.* **33**, 1553–63 (2005).
37. Shigemoto, K. *et al.* Identification and characterisation of a developmentally regulated mammalian gene that utilises -1 programmed ribosomal frameshifting. *Nucleic Acids Res.* **29**, 4079–88 (2001).
38. Ten Dam, E. B., Pleij, C. W. & Bosch, L. RNA pseudoknots: translational frameshifting and readthrough on viral RNAs. *Virus Genes* **4**, 121–36 (1990).
39. Marczinke, B., Hagervall, T. & Brierley, I. The Q-base of asparaginyl-tRNA is dispensable for efficient -1 ribosomal frameshifting in eukaryotes. *J. Mol. Biol.* **295**, 179–91 (2000).
40. Dinman, J. D. & Wickner, R. B. Ribosomal frameshifting efficiency and gag/gag-pol ratio are critical for yeast M1 double-stranded RNA virus propagation. *J. Virol.* **66**, 3669–76 (1992).

41. Dinman, J. D. Mechanisms and implications of programmed translational frameshifting. *Wiley Interdiscip. Rev. RNA* **3**, 661–73 (2012).
42. Belcourt, M. F. & Farabaugh, P. J. Ribosomal frameshifting in the yeast retrotransposon Ty: tRNAs induce slippage on a 7 nucleotide minimal site. *Cell* **62**, 339–52 (1990).
43. Farabaugh, P. J., Zhao, H. & Vimaladithan, A. A novel programmed frameshift expresses the POL3 gene of retrotransposon Ty3 of yeast: frameshifting without tRNA slippage. *Cell* **74**, 93–103 (1993).
44. Clare, J. & Farabaugh, P. Nucleotide sequence of a yeast Ty element: evidence for an unusual mechanism of gene expression. *Proc. Natl. Acad. Sci. U. S. A.* **82**, 2829–33 (1985).
45. Allmang, C. & Krol, A. Selenoprotein synthesis: UGA does not end the story. *Biochimie* **88**, 1561–71 (2006).
46. Dinman, J. D. Control of gene expression by translational recoding. *Adv. Protein Chem. Struct. Biol.* **86**, 129–49 (2012).
47. Hansen, J. L., Moore, P. B. & Steitz, T. a. Structures of five antibiotics bound at the peptidyl transferase center of the large ribosomal subunit. *J. Mol. Biol.* **330**, 1061–1075 (2003).
48. Léger-Silvestre, I. *et al.* The ribosomal protein Rps15p is required for nuclear exit of the 40S subunit precursors in yeast. *EMBO J.* **23**, 2336–47 (2004).
49. Schwarzbauer, J. & Craven, G. R. Evidence that E. coli ribosomal protein S13 has two separable functional domains involved in 16S RNA recognition and protein S19 binding. *Nucleic Acids Res.* **13**, 6767–6786 (1985).
50. Khairulina, J. *et al.* Eukaryote-specific motif of ribosomal protein S15 neighbors A site codon during elongation and termination of translation. *Biochimie* **92**, 820–5 (2010).
51. Cukras, A. R. & Green, R. Multiple effects of S13 in modulating the strength of intersubunit interactions in the ribosome during translation. *J. Mol. Biol.* **349**, 47–59 (2005).
52. Rakauskaitė, R. & Dinman, J. D. An arc of unpaired “hinge bases” facilitates information exchange among functional centers of the ribosome. *Mol. Cell. Biol.* **26**, 8992–9002 (2006).

53. Grondek, J. F. & Culver, G. M. Assembly of the 30S ribosomal subunit: positioning ribosomal protein S13 in the S7 assembly branch. *RNA* **10**, 1861–1866 (2004).
54. Zhang, W., Dunkle, J. A. & Cate, J. H. D. Structures of the ribosome in intermediate states of ratcheting. *Science* **325**, 1014–7 (2009).
55. Frank, J. Intermediate states during mRNA-tRNA translocation. *Curr. Opin. Struct. Biol.* **22**, 778–85 (2012).
56. Musalgaonkar, S., Moomau, C. A. & Dinman, J. D. Ribosomes in the balance: structural equilibrium ensures translational fidelity and proper gene expression. *Nucleic Acids Res.* **42**, 13384–13392 (2014).
57. Sulima, S. O. *et al.* Eukaryotic rpL10 drives ribosomal rotation. *Nucleic Acids Res.* **42**, 2049–63 (2014).
58. Ratje, A. H. *et al.* Head swivel on the ribosome facilitates translocation by means of intra-subunit tRNA hybrid sites. *Nature* **468**, 713–6 (2010).
59. Cukras, a. R., Southworth, D. R., Brunelle, J. L., Culver, G. M. & Green, R. Ribosomal proteins S12 and S13 function as control elements for translocation of the mRNA: tRNA complex. *Mol. Cell* **12**, 321–328 (2003).
60. Dubnau, E., Soares, S., Huang, T. J. & Jacobs, W. R. Overproduction of mycobacterial ribosomal protein S13 induces catalase/oxidase activity and hypersensitivity to isoniazid in *Mycobacterium smegmatis*. *Gene* **170**, 17–22 (1996).
61. Rhodin, M. H. J. & Dinman, J. D. A flexible loop in yeast ribosomal protein L11 coordinates P-site tRNA binding. *Nucleic Acids Res.* **38**, 8377–89 (2010).
62. Taylor, D. J. *et al.* Comprehensive molecular structure of the eukaryotic ribosome. *Structure* **17**, 1591–604 (2009).
63. Vasa, S. M., Guex, N., Wilkinson, K. A., Weeks, K. M. & Giddings, M. C. ShapeFinder: a software system for high-throughput quantitative analysis of nucleic acid reactivity information resolved by capillary electrophoresis. *RNA* **14**, 1979–90 (2008).
64. Kaczanowska, M. & Rydén-Aulin, M. Ribosome biogenesis and the translation process in *Escherichia coli*. *Microbiol. Mol. Biol. Rev.* **71**, 477–94 (2007).
65. Passmore, L. A. *et al.* The eukaryotic translation initiation factors eIF1 and eIF1A induce an open conformation of the 40S ribosome. *Mol. Cell* **26**, 41–50 (2007).

66. Nakamoto, T. The initiation of eukaryotic and prokaryotic protein synthesis: a selective accessibility and multisubstrate enzyme reaction. *Gene* **403**, 1–5 (2007).
67. Boni, I. V. [Diverse molecular mechanisms for translation initiation in prokaryotes]. *Mol. Biol. (Mosk)*. **40**, 658–68 (2006).
68. Cheung, Y. N. *et al.* Dissociation of eIF1 from the 40S ribosomal subunit is a key step in start codon selection in vivo. *Genes Dev.* **21**, 1217–1230 (2007).
69. Ito, H., Fukuda, Y., Murata, K. & Kimura, A. Transformation of intact yeast cells treated with alkali cations. *J. Bacteriol.* **153**, 163–8 (1983).
70. Maniatis, T., Fritsch, E. F. & Sambrook, J. *Molecular cloning: a laboratory manual*. 545 (Cold Spring Harbor Laboratory, 1982).
71. Jacobs, J. L. & Dinman, J. D. Systematic analysis of bicistronic reporter assay data. *Nucleic Acids Res.* **32**, e160 (2004).
72. Meskauskas, A. & Dinman, J. D. A molecular clamp ensures allosteric coordination of peptidyltransfer and ligand binding to the ribosomal A-site. *Nucleic Acids Res.* **38**, 7800–13 (2010).
73. Ortiz, P. a., Ulloque, R., Kihara, G. K., Zheng, H. & Kinzy, T. G. Translation elongation factor 2 anticodon mimicry domain mutants affect fidelity and diphtheria toxin resistance. *J. Biol. Chem.* **281**, 32639–32648 (2006).
74. Belew, A. T., Advani, V. M. & Dinman, J. D. Endogenous ribosomal frameshift signals operate as mRNA destabilizing elements through at least two molecular pathways in yeast. *Nucleic Acids Res.* **39**, 2799–808 (2011).